Robotica (2013) volume 31, pp. 423–439. © Cambridge University Press 2012
doi:10.1017/S0263574712000458

Modeling and robust backstepping control of an underactuated quadruped robot in bounding motion

Hamed Kazemi†, Vahid Johari Majd†* and Majid M. Moghaddam‡

†*Intelligent Control Systems Laboratory, School of Electrical and Computer Engineering, Tarbiat Modares University, P.O. Box 14115-194, Tehran, Iran*
‡*Robotics and Mechatronics Laboratory, Mechanical Engineering Department, Tarbiat Modares University, Tehran, Iran*

(Accepted July 18, 2012. First published online: August 14, 2012)

SUMMARY
In this paper, a model-based exponential stabilization of a quadruped robot is studied in bounding motion. The dynamics of the five-link planar underactuated mechanical model of the quadruped robot with four actuated joints system is derived. It is shown that the dynamical equation of the proposed simplified model belongs to a class of second-order nonholonomic mechanical systems which cannot be stabilized by any smooth time-invariant state feedback. Utilizing a coordinate transformation based on the so-called normalized momentum, a robust backstepping control method is presented for the quadruped robot. Both theoretical analysis and numerical simulations show that the robust backstepping controller can stabilize the underactuated quadruped robot so that it could balance on its rear legs and track a desired trajectory. Despite the model parameter uncertainties, the robustness of the controller is maintained. The simulation results show the effectiveness of the proposed method.

KEYWORDS: Quadruped robot; Lagrangian modeling; Underactuated system; Nonholonomic system; Nonlinear control.

1. Introduction

The legged robots are an important class of biologically inspired robotic systems, which have been investigated by many researchers in the past three decades.[1,2] The quadruped robots due to their similar capabilities with the natural walking/running animals have attracted much attention in recent years. Little-Dog is a successful example of such robots, which can move in rough terrain and climb from obstacles with walking and bounding gaits.[3] Bounding gait is a dynamic motion that the robot stands in two legs. This is a challenging task for quadruped robot since the robot is underactuated in this stance. The presence of unactuated joints results in a complicated dynamical relationship between the actuated joints and the ground.

Underactuated Mechanical Systems are those systems that have more degrees of freedom (DOF) than the actuators.[4,5] The mechanical underactuated systems are often called second-ordered nonholonomic system.[6,7] An underactuated mechanical system is generally nonlinear in nature, and cannot be globally linearized by static or dynamic feedback[8] except for the differentially flat systems. However, one can employ famous Brockett's theorem[9] to transform such systems to special normal forms. Stabilizing nonlinear systems without a special normal form is generally an open problem.[10] Recently, the main progresses for the nonlinear control theory highly depend on the nonlinear systems that holding special geometric or algebraic structures,[11] such as the strict feedback normal form[4] or feedforward normal forms.[12,13] The former can be stabilized by the backstepping procedure[14] and the latter can be stabilized by state feedback in explicit form as nested saturations.[12] For nonholonomic system, if the control distribution of the system has nilpotent property,[15] the system can be transformed into a triangular normal form.[16,17] However, a general solution to obtain the transformation for any nonlinear system does not exist. Therefore, an approximate normal form transformation combining with a robust control may be adopted. This method has been employed for balancing a one-leg hopping robot with two arms.[18] However, one-leg hopping robot has much simple dynamic model compared to quadruped robot.

For controlling the underactuated mechanical systems, Olfati-Saber presented a method in ref. [10] called normalized momentum. If the underactuated system has symmetric kinetic energy, one can change the partially linearized form of the dynamics into a special case of the famous Byrnes–Isidori normal forms,[4] namely strict feedback and feedforward forms, with a double integrator, such that the control input does not appear in the unactuated subsystem. This simplifies the control design by reducing the control of the original higher order system into the control of its lower order nonlinear unactuated subsystem.

Backstepping control is an effective control technique which is especially used for a class of nonlinear systems that are strict feedback form transformable.[14,19] In works such as refs. [4, 19], the authors have made significant contributions to the development of this theory. Moreover, in ref. [18], this theory has been used for robust control of a hopping robot in stance phase with two active and two passive joints.

In this paper, a new simplified dynamic model of underactuated quadruped robot in bounding motion with four actuated and two unactuated joints is developed for the first time using the Lagrangian method. Based on the Olfati-Saber coordinate transformation given in ref. [10], an

* Corresponding author. E-mail: majd@modares.ac.ir

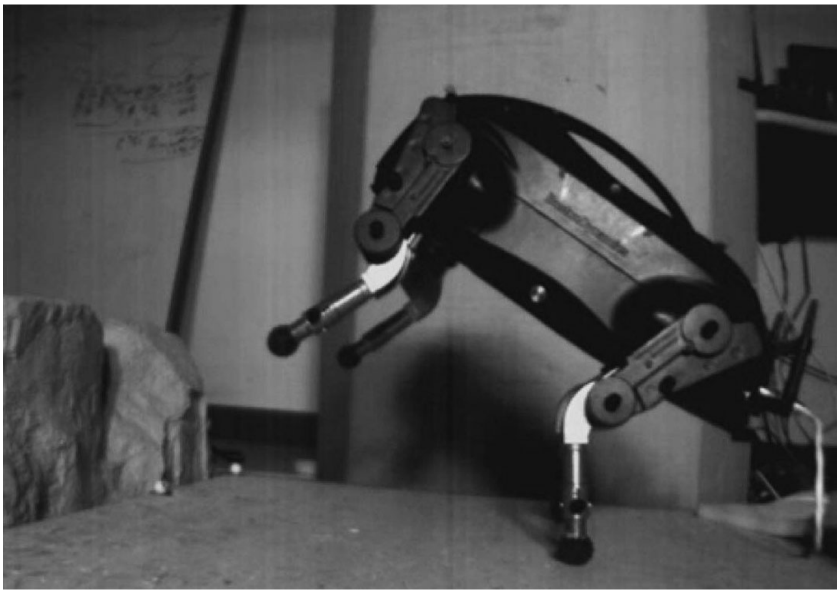

Fig. 1. Little-Dog robot in the bounding motion.[3]

approximate normal form of the model is obtained. Then, a robust backstepping controller is employed for this system. The approximated transformation introduces uncertainties in the simplified dynamical model. Despite the model and parameter uncertainty, the robustness of the controller is maintained while achieving proper performance. It is shown that the proposed controller stabilizes the underactuated quadruped robot and allows tracking the desired trajectory in bounding motion in a suitable range.

The paper is organized as follows. In Section 2, the robot model is introduced and the dynamics of the robot are analyzed. In Section 3, an approximate strict feedback normal form with perturbation terms is presented based on the transformation mentioned in ref. [10]. Since the approximations introduce some uncertainties into the model, a robust backstepping controller is used in Section 4. Section 5 presents some numerical simulations that verify the suggested schemes in the former two sections. Finally, the concluding remarks are provided in Section 6.

2. Dynamics of the Underactuated Quadruped Robot in Bounding Motion

Obtaining an accurate dynamic model for quadruped robot has proven to be quite difficult due to its high DOF and its ground interactions. The complications are more pronounced in the bounding motion compared to walking gates. Figure 1 shows a quadruped robot known as Little-Dog in bounding motion.[3] The Little-Dog robot has 12 actuators: two in each hip and one in each knee for each leg. When the robot moves in the three-dimensional space, it will have 22 DOF: six for the body, three rotational joints in each leg, and one prismatic spring in each leg. By assuming that the leg springs are overdamped and has first-order dynamics, we arrive at a 40-dimensional state space ($18 \times 2 + 4$).

According to the Little-Dog properties as a sample, quadruped robot is a complicated system. However, to keep the model as simple and low dimensional as possible, we

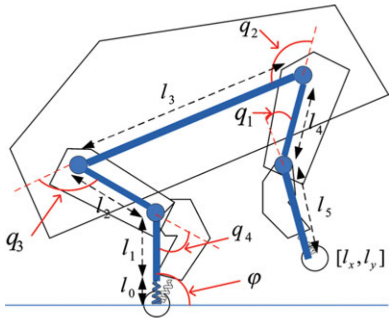

Fig. 2. (Colour online) Quadruped robot planar model in bounding motion.

approximate the dynamics of the quadruped robot using a planar five-link serial rigid-body chain model for bounding motion, with revolute joints connecting the links, and a free base joint, as shown in Fig. 2. Due to lateral symmetry in the planar model, only one side of the body needs to be considered. In other words, it is assumed that the rear legs (feet) move together as one and the front legs (hands) move together as one. We assume like Little-Dog the robot leg has two segments: the shin and the upper leg. The shin itself consists of rigid parts and a massless stiff spring which moves along the axis of the shin. For bounding motion, the connection between the ground and foot of the quadruped robot is considered as a passive joint. The spring is another passive DOF.

Let the generalized coordinates of the planar model be $(\varphi, l_0, q_1, q_2, q_3, q_4)$, where φ is the angle between leg's axis and the ground, l_0 is the length of massless shin ($l_0 = l_{00}$ when spring is free), and q_1, q_2, q_3, q_4 are angular variables of between the links, respectively. Positive direction of q_2, q_3 is assumed to be clockwise and other angles are counter-clockwise. In bounding locomotion, we want to move the position of the hand (l_x, l_y) to desired point. The length of the rigid part of the shin with nonzero mass is $l_1$with mass m_1. The massless segment that has the length l_0 serially

https://doi.org/10.1017/S0263574712000458 Published online by Cambridge University Press

connected to the former. The stiffness of the linear spring is k.

The planar model shown in Fig. 2 has six DOF in bounding phase and is actuated by four actuators on the joints. Thus, the telescopic and swing motions of the robot leg are due to the dynamics coupling of the four links indirectly.

The generalized coordinates in bounding phase can be denoted by $x = [x_p^T, x_a^T]^T$,where $x_p = [l_0, \varphi]^T$ and $x_a = [q_1, q_2, q_3, q_4]^T$ correspond to the passive and the active joints, respectively. The Lagrangian of the planar model is of the form

$$L(x, \dot{x}) = K(x, \dot{x}) - V(x) = \frac{1}{2}\begin{bmatrix}\dot{x}_p\\ \dot{x}_a\end{bmatrix}^T M(x_p, x_a)\begin{bmatrix}\dot{x}_p\\ \dot{x}_a\end{bmatrix} - V(x), \quad (1)$$

where K and V denote the kinetic and potential energies, respectively. The inertia matrix $M(x_p, x_a)$ can be written as

$$M(x_p, x_a) = \begin{bmatrix} M_{pp} & M_{pa}\\ M_{ap} & M_{aa}\end{bmatrix}, \quad (2)$$

whose submatrices are obtained in Appendix A. One can see from the appendix that the inertia matrix is only a function of variables $(l_0, q_1, q_2, q_3, q_4)$ and is independent of variable φ. This follows that $K(x, \dot{x})$ is also independent of φ. According to Lagrangian mechanics, if the Lagrangian function $L(x, \dot{x})$ is independent of a generalized coordinates x_i, then one can say that the Lagrangian is symmetric with respect to x_i. In this case, x_i is said to be a cyclic coordinates.[10] Lagrangian symmetry gives identical equation as

$$\partial L(x, \dot{x})/\partial x_i = 0. \quad (3)$$

For a mechanics system, the Lagrangian dynamics has an expression

$$\frac{d}{dt}\frac{\partial L(x, \dot{x})}{\partial \dot{x}_i} - \frac{\partial L(x, \dot{x})}{\partial x_i} = \tau_i. \quad (4)$$

For a pure system (without any controls), τ_i is equal to zero. Considering Eq. (3), Eq. (4) reduces to

$$p_i = \partial L(x, \dot{x})/\partial \dot{x}_i = \text{constant}. \quad (5)$$

This means that p_i is a conserved quantity. For the underactuated planar model shown in Fig. 2, one can verify that the potential energy of the robot is a function of all generalized coordinates such that there is no Lagrangian symmetry. However, as mentioned above, the kinetic energy $K(x, \dot{x})$ is symmetric with respect to variable φ, and thus one can write

$$\partial K(x, \dot{x})/\partial \varphi = 0. \quad (6)$$

Since the robot has a nonconstant potential energy, the existence of kinetic symmetry does not lead to existence of conserved quantities. In control viewpoint, the existence of conserved quantities always leads to losing the controllability of the system, which is a typical case for underactuated systems.

Considering the kinetic symmetry and utilizing Eq. (4), the Lagrangian dynamics of the planar model can be expressed as

$$\begin{aligned} &\frac{d}{dt}\frac{\partial K}{\partial \dot{l}_0} - \frac{\partial L}{\partial l_0} = 0,\\ &\frac{d}{dt}\frac{\partial K}{\partial \dot{\varphi}} + \frac{\partial V}{\partial \varphi} = 0,\\ &\frac{d}{dt}\frac{\partial K}{\partial \dot{q}_i} - \frac{\partial L}{\partial q_i} = \tau_i, \quad i = 1, \ldots, 4, \end{aligned} \quad (7)$$

where $\tau_i, i = 1, \ldots, 4$ is the joint torque. The first two equations of Eq. (7), with right-hand side zero can be considered as differential constraints of the actuated part. Since $\partial L/\partial l_0 \neq 0$ and $\partial L/\partial \varphi \neq 0$, the first two equations of Eq. (7) cannot be reduced to a first-order or an algebraic equation, and therefore, system (7) is a second-order nonholonomic system. From the above discussions, one can conclude that:

(a) The planar model of the quadruped robot is an underactuated mechanical system since the six DOF mechanical system has only four actuators.
(b) The planar model is a second-order nonholonomic system because of the nonconstant potential field.
(c) The planar model has no Lagrangian symmetry but has kinetic symmetry. This plays a vital role in the controllability and stabilization of the underactuated system.

3. Deriving the Normal Form of the Dynamics

In this section, we transform the underactuated system (7) into a normal form such that the control problem can be resolved effectively. Using Appendix A in finding the derivatives in Eq. (7), one can write the model as

$$\begin{aligned} m_{pp}\ddot{x}_p + m_{pa}\ddot{x}_a + c_p(x, \dot{x}) = 0,\\ m_{ap}\ddot{x}_p + m_{aa}\ddot{x}_a + c_a(x, \dot{x}) = \tau, \end{aligned} \quad (8)$$

where the terms $c_p(x, \dot{x})$ and $c_a(x, \dot{x})$ both include the centrifugal, Coriolis, gravitational, and frictional forces, which can be found from Eq. (7). Since m_{pp} is invertible (see Appendix A), using a partial feedback linearization of the form

$$\tau = \left(m_{aa} - m_{ap}m_{pp}^{-1}m_{pa}\right)\ddot{x}_a + \left(c_a - m_{ap}m_{pp}^{-1}c_p\right), \quad (9)$$

and defining u as

$$u = \left(m_{aa} - m_{ap}m_{pp}^{-1}m_{pa}\right)^{-1}\left(\tau - c_a + m_{ap}m_{pp}^{-1}c_p\right), \quad (10)$$

system (8) is transformed into a partially linearized form

$$\begin{aligned} \dot{x}_p &= y_p,\\ \dot{y}_p &= -m_{pp}^{-1}c_p - m_{pp}^{-1}m_{pa}u, \end{aligned} \quad (11)$$

https://doi.org/10.1017/S0263574712000458 Published online by Cambridge University Press

$$\dot{x}_a = y_a,$$
$$\dot{y}_a = u,$$

where $u = \ddot{x}_a$ is considered as the new input. Obviously, subsystem (x_a, y_a) is linearized whereas subsystem (x_p, y_p) remains highly nonlinear, and the new control u appears in both subsystems. In fact, the existence of the control signal in nonlinear subsystem highly increases the complexity of control design for underactuated systems.

In order to transform system (11) into a normalized form, at first we bring the Olfati-Saber transformation along with some necessary definitions in this regard, and we apply them to this model.

Definition 1. External variables and shape variables[10]**:** The variables that appear in the kinetic energy of the mechanical system with Lagrangian (1) are called shape variables. A configuration variable is called an external variable, if it does not appear in the kinetic energy, i.e., $\partial K(x,\dot{x})/\partial x_i = 0$.

Definition 2. Normalized momentum[10]**:** For the underactuated system (8), the normalized momentum with respect to the generalized coordinates x_p,x_a are defined as

$$\begin{aligned}\pi_p &= m_{pp}^{-1}\frac{\partial L}{\partial \dot{x}_p} = \dot{x}_p + m_{pp}^{-1}m_{pa}\dot{x}_a,\\ \pi_a &= m_{pa}^{-1}\frac{\partial L}{\partial \dot{x}_a} = \dot{x}_a + m_{pa}^{-1}m_{aa}\dot{x}_p,\end{aligned} \tag{12}$$

respectively.

Definition 3. Strict feedback form[10]**:** A nonlinear system is said to be in strict feedback form if it has the following triangular structure:

$$\begin{aligned}\dot{z} &= f(z,\gamma_1),\\ \dot{\gamma}_1 &= \gamma_2,\\ &\cdots\\ \gamma_m &= u.\end{aligned} \tag{13}$$

The following proposition gives the condition for transforming the underactuated mechanical system to the strict feedback normal form, so that the system can be stabilized by the backstepping procedure.[19]

Proposition 1. Strict feedback form transformation[10]**:** Assume that the unactuated coordinates x_p are external variables and the actuated coordinates x_a are shape variables. If the normalized momentum π_p in Eq. (12) is integrable and the part $\omega = [m_{pp}^{-1}(x_a)m_{pa}(x_a)]dx_a$ of π_p has the form $\omega = d\Im(x_a)$, then there exists a global coordinate transformation of the form

$$\begin{aligned}x_r &= x_p + \Im(x_a),\\ y_r &= \partial L/\partial \dot{x}_p = m_{pp}(x_a)\dot{x}_p + m_{pa}(x_a)\dot{x}_a,\end{aligned} \tag{14}$$

that along with partial feedback linearization (9) transforms the dynamics of the system (8) into the following cascade nonlinear system in a strict feedback form:

$$\begin{aligned}\dot{x}_r &= m_{pp}^{-1}(x_a)y_r,\\ \dot{y}_r &= -\tfrac{\partial V(x_r-\Im(x_a),x_a)}{\partial x_r},\\ \dot{x}_a &= y_a,\\ \dot{y}_a &= u,\end{aligned} \tag{15}$$

where $u = \ddot{x}_a$ is the new input.

Remark 1: The planar model with Eq. (7) does not satisfy the condition of **Proposition 1** since the passive coordinate l_0 is not a kinetic symmetrical coordinate. However, as shown in the following two propositions, system (7) can be approximated to satisfy the conditions of **Proposition 1**.

Extending of **Proposition 1** to hold for any mechanical system with nonsymmetric kinetic energy with respect to passive variables that can be approximated by desired constants, we provide the following proposition.

Proposition 2. Approximate momentum integral: Consider the dynamics of the underactuated quadruped planar model (7), if the kinetic energy $K(l_0,q_1,q_2,q_3,q_4)$ is estimated by $\hat{K}(l_{01},q_1,q_2,q_3,q_4)$, i.e., $l_0 \approx l_{01}$, then it follows that:

(a) The approximate kinetic energy $\hat{K}(l_{01},q_1,q_2,q_3,q_4)$ is symmetric about the passive coordinates $x_p = [l_0,\varphi]^T$.
(b) If the matrix $\hat{m}_{pp}(l_{01},q_1,q_2,q_3,q_4)$ is estimated by $\hat{m}_{pp}(l_{01},q_1^*,q_2^*,q_3^*,q_4^*)$, in which $q_i^*, i = 1,2,3,4$ are any given angular positions of the four links, respectively, then the approximate momentum part $\hat{\omega} = [\hat{m}_{pp}^{-1}(l_{01},q_1^*,q_2^*,q_3^*,q_4^*)\hat{m}_{pa}(l_{01},q_1,q_2,q_3,q_4)]dx_a$ is integrable.

Proof.

(a) Considering Appendix A, by letting $l_0 \approx l_{01}$, it is trivial that the approximate kinetic energy $\hat{K}(l_{01},q_1,q_2,q_3,q_4)$ becomes independent of passive coordinates $x_p = [l_0,\varphi]^T$, which makes it is symmetric about x_p.
(b) Let $\hat{m}_{pp}(l_{01},q_1,q_2,q_3,q_4) \approx \hat{m}_{pp}(l_{01},q_1^*,q_2^*,q_3^*,q_4^*)$, referring to Appendix A, the approximate momentum part can be written as

$$\begin{aligned}\hat{\omega} &= \left[\hat{m}_{pp}^{-1}(l_{01},q_1^*,q_2^*,q_3^*,q_4^*)\hat{m}_{pa}(l_{01},q_1,q_2,q_3,q_4)\right]dx_a\\ &= \hat{m}_{pp}^{-1}(l_{01},q_1^*,q_2^*,q_3^*,q_4^*)\\ &\quad\times\begin{bmatrix}M_{13}dq_1 + M_{14}dq_2 + M_{15}dq_3 + M_{16}dq_4\\ M_{23}dq_1 + M_{24}dq_2 + M_{25}dq_3 + M_{26}dq_4\end{bmatrix},\end{aligned} \tag{16}$$

where according to Appendix A, M_{ij} $(i = 1,2 \& j = 3,4,5,6)$ is a function of q_i $(i = 1,2,3,4)$. This can be denoted by $\hat{\omega} = d\Im(l_{01},q_1,q_2,q_3,q_4)$. Then, it follows that:

$$\Im(l_{01},q_1,q_2,q_3,q_4) = \hat{m}_{pp}^{-1}(l_{01},q_1^*,q_2^*,q_3^*,q_4^*)\begin{bmatrix}\wp_{11}\\ \wp_{12}\end{bmatrix}, \tag{17}$$

where $\wp_{1j}$ $(j = 1,2)$ is the integral of $\hat{m}_{pa}(l_{01},q_1,q_2,q_3,q_4)$ and can directly be obtained. This completes the proof. □

https://doi.org/10.1017/S0263574712000458 Published online by Cambridge University Press

Remark 2: When using **Proposition 1** along with **Proposition 2** to transform an underactuated system into the strict feedback form, the resulting approximation error should be taken into account. Considering the Lagrangian (1), since the potential energy $V(x)$ is only a function of generalized coordinates (i.e., $\partial V(x)/\partial \dot{x} = 0$), the generalized momentum given in Eq. (14) can be written as

$$\frac{\partial L(x,\dot{x})}{\partial \dot{x}} = \frac{\partial K(x,\dot{x})}{\partial \dot{x}} - \frac{\partial V(x)}{\partial \dot{x}} = \frac{\partial K(x,\dot{x})}{\partial \dot{x}} = M(x)\dot{x}. \tag{18}$$

The momentum part is relative to the passive coordinates, i.e.

$$y_r = \partial L/\partial \dot{x}_p = m_{pp}(x)\dot{x}_p + m_{pa}(x)\dot{x}_a. \tag{19}$$

Considering the approximations $l_0 \approx l_{01}$ and $m_{pp}(l_0, q_1, q_2, q_3, q_4) \approx \hat{m}_{pp}(l_{01}, q_1^*, q_2^*, q_3^*, q_4^*)$, then the approximate momentum in Eq. (16) can be expressed by

$$\hat{y}_r = \hat{m}_{pp}(l_{01}, q_1^*, q_2^*, q_3^*, q_4^*)\dot{x}_p + \hat{m}_{pa}(l_{01}, q_1, q_2, q_3, q_4)\dot{x}_a. \tag{20}$$

For systems that satisfy the conditions of **Proposition 1** and **Proposition 2**, we present the following proposition which shows that the underactuated system (8) can be transformed into a strict feedback normal form with perturbation terms such that the nonlinear dynamic system (8) can be controlled by robust backstepping procedure.

Proposition 3. Strict feedback form with perturbation terms: For the underactuated planar model (8), combining partial feedback linearization (9), the new control signal (10) and the following coordinate transformation:

$$\begin{aligned} x_r &= x_p + \Im(l_{01}, q_1, q_2, q_3, q_4), \\ y_r &= \partial L/\partial \dot{x}_p = m_{pp}(x_a)\dot{x}_p + m_{pa}(x_a)\dot{x}_a, \end{aligned} \tag{21}$$

transforms system (8) into the following strict feedback form:

$$\begin{aligned} \dot{x}_r &= \hat{m}_{pp}^{-1}(l_{01}, q_1^*, q_2^*, q_3^*, q_4^*)y_r + \varepsilon_1, \\ \dot{y}_r &= -\frac{\partial V(x_r - \Im(l_{01}, q_1, q_2, q_3, q_4), x_a)}{\partial x_r} + \varepsilon_2, \\ \dot{x}_a &= y_a, \\ \dot{y}_a &= u, \end{aligned} \tag{22}$$

with perturbations terms given by

$$\varepsilon_1 = \hat{y}_r - y_r,\ \varepsilon_2 = \begin{bmatrix} \partial K/\partial l_0 \\ 0 \end{bmatrix}. \tag{23}$$

Proof. Using Eqs. (9) and (10), system (8) reduces to

$$\begin{aligned} m_{pp}\ddot{x}_p + m_{pa}\ddot{x}_a + c_p(x,\dot{x}) &= 0, \\ \dot{x}_a &= y_a, \\ \dot{y}_a &= u. \end{aligned} \tag{24}$$

Thus, the last two equations of Eq. (22) are verified. Moreover, substituting Eqs. (21) and (16) into the left-hand side of the first equation in Eq. (22) yields

$$\begin{aligned} \dot{x}_r &= \dot{x}_p + \frac{d}{dt}\Im(l_{01}, q_1, q_2, q_3, q_4) \\ &= \dot{x}_p + \hat{m}_{pp}^{-1}(l_{01}, q_1^*, q_2^*, q_3^*, q_4^*)\hat{m}_{pa}(l_{01}, q_1, q_2, q_3, q_4)\dot{x}_a \\ &= \hat{m}_{pp}(l_{01}, q_1^*, q_2^*, q_3^*, q_4^*)(y_r + \varepsilon_1), \end{aligned} \tag{25}$$

where $\varepsilon_1 = \hat{y}_r - y_r$, which proves the first equation of Eq. (22). To prove the second equation of Eq. (22), consider the first two equations of Eq. (7). Since $\partial V/\partial \dot{x}_p = 0$, one can write

$$\frac{d}{dt}\left(\frac{\partial L}{\partial \dot{x}_p}\right) = -\frac{\partial V}{\partial x_p} + \begin{bmatrix} \partial K/\partial l_0 \\ 0 \end{bmatrix}. \tag{26}$$

Using Eq. (19) in Eq. (26) gives

$$\dot{y}_r = -\frac{\partial V}{\partial x_p} + \begin{bmatrix} \partial K/\partial l_0 \\ 0 \end{bmatrix}. \tag{27}$$

Let $\varepsilon_2 = \begin{bmatrix} \partial K/\partial l_0 \\ 0 \end{bmatrix}$. Equations (26) and (27) follow that:

$$\dot{y}_r = -\partial V/\partial x_p + \varepsilon_2. \tag{28}$$

The first equation in Eq. (21) implies that $\frac{\partial x_r}{\partial x_p} = I$, so one can write

$$\frac{\partial V(x_p, x_a)}{\partial x_p} = \frac{\partial V(x_r - \Im(l_{01}, q_1, q_2, q_3, q_4), x_a)}{\partial x_r}. \tag{29}$$

Therefore, Eq. (28) reduces to

$$\dot{y}_r = -\frac{\partial V(x_r - \Im(l_{01}, q_1, q_2, q_3, q_4), x_a)}{\partial x_r} + \varepsilon_2. \tag{30}$$

Hence, the second equation of Eq. (22) is verified, which completes the proof. □

Remark 3: Letting $(z_1, z_2) = (x_r, y_r)$ and $(\gamma_1, \gamma_2) = (x_a, y_a)$, Eq. (22) can be rewritten in a more familiar form as

$$\begin{aligned} \dot{z} &= f(z, \gamma_1, \varepsilon), \\ \dot{\gamma}_1 &= \gamma_2, \\ \dot{\gamma}_2 &= u. \end{aligned} \tag{31}$$

The normal form (31) with nonlinear perturbation ε indicates that the standard backstepping procedure cannot be used directly, and thus a robust backstepping controller is necessary.

4. Robust Backstepping Control

In this section, we present a robust controller for system (22). To allow the proposed controller fit both the set-point regulation and trajectory tracking tasks, we employ transformation: $z_1 = x_r^d - x_r$, $z_2 = y_r^d - y_r$,

https://doi.org/10.1017/S0263574712000458 Published online by Cambridge University Press

$\gamma_1 = x_a^d - x_a$, $\gamma_2 = y_a^d - y_a$ on system (22), where the superscript d denotes the desired trajectory of the corresponding variable. Therefore, Eq. (22) reduces to

$$\begin{aligned}
\dot{z}_1 &= \dot{x}_r^d - \hat{m}_{pp}^{-1}(l_{01}, q_1^*, q_2^*, q_3^*, q_4^*)(y_r^d - z_2) - \varepsilon_1,\\
\dot{z}_2 &= \dot{y}_r^d - f_r(x_r^d - z_1, x_a^d - \gamma_1) - \varepsilon_2,\\
\dot{\gamma}_1 &= \gamma_2,\\
\dot{\gamma}_2 &= \dot{y}_a^d - u,
\end{aligned} \tag{32}$$

where

$$f_r(x_r, x_a) = -\frac{\partial V(x_r - \Im(l_{01}, q_1, q_2, q_3, q_4), x_a)}{\partial x_r}.$$

It can be seen that in the z-subsystem of Eq. (32), function f_r is not affine with respect to the input variableγ_1. Although a backstepping theorem for the nonaffine system has already been developed in ref. [4], it has some restrictive conditions that make it difficult to find a Lyapunov function. Therefore, we would prefer to find an affine approximation of function f_r for system (32). Referring to Eq. (29) and Appendix A, one can write

$$f_r(x_r, x_a) = -\frac{\partial V(x_p, x_a)}{\partial x_p} = [f_{r_1} \quad f_{r_2}]^T, \tag{33}$$

where

$$\begin{aligned}
f_{r_1} &= -\frac{\partial V}{\partial l_0} = -(m_1 + m_2 + m_3 + m_4 + m_5)g \sin\varphi\\
&\quad - k(l_0 - l_{00}),\\
f_{r_2} &= -\frac{\partial V}{\partial \varphi} = -[(l_0 + l_{10})m_1 + (l_0 + l_1)(m_2 + m_3 + m_4\\
&\quad + m_5)]g \cos\varphi - [l_{20}m_2 + l_2(m_3 + m_4 + m_5)]g \cos(\varphi\\
&\quad + q_4) - [l_{30}m_3 + l_3(m_4 + m_5)]g \cos(\varphi + q_3 + q_4)\\
&\quad - [l_{40}m_4 + l_4 m_5]g \cos(\varphi + q_2 + q_3 + q_4)\\
&\quad - l_{50}m_5 g \cos(\varphi + q_1 + q_2 + q_3 + q_4).
\end{aligned}$$

Obviously, in the above equations, functions f_{r_1} and f_{r_2} are not affine in variables $\gamma_1 = x_a = [q_1, q_2, q_3, q_4]^T$, one may consider the motion of leg near to the vertical position at the bounding motion, which implies that $\varphi \approx \pi/2$, and consequently, $\sin\varphi \approx 1$, $\cos\varphi \approx 0.5\pi - \varphi$, $\cos(\varphi + \alpha) \approx -\sin\alpha$. In addition, let $l_0 \approx l_{01}$ in f_{r_2} then f_{r_1} and f_{r_2} can be estimated by

$$\begin{aligned}
\hat{f}_{r_1} &= -(m_1 + m_2 + m_3 + m_4 + m_5)g - k(l_0 - l_{00}),\\
\hat{f}_{r_2} &= F_0 g(\varphi - 0.5\pi) + [l_{20}m_2 + l_2(m_3 + m_4 + m_5)]g \sin(q_4)\\
&\quad + [l_{30}m_3 + l_3(m_4 + m_5)]g \sin(q_3 + q_4) + [l_{40}m_4\\
&\quad + l_4 m_5]g \sin(q_2 + q_3 + q_4) + l_{50}m_5 g \sin(q_1 + q_2\\
&\quad + q_3 + q_4),
\end{aligned} \tag{34}$$

where $F_0 = (l_0 + l_{10})m_1 + (l_0 + l_1)(m_2 + m_3 + m_4 + m_5)$. Substituting Eq. (17) into Eq. (21) yields

$$x_r = \begin{bmatrix} l_0 \\ \varphi \end{bmatrix} + \hat{m}_{pp}^{-1}(l_{01}, q_1^*, q_2^*, q_3^*, q_4^*) \begin{bmatrix} \wp_{11} \\ \wp_{12} \end{bmatrix}. \tag{35}$$

Using Eq. (35) in Eq. (34) and considering the first-order approximation of $\sin(\cdot)$, the estimate of f_r can be expressed as

$$\begin{aligned}
\hat{f}_r &= f_0(x_r, l_{01}, q_1^*, q_2^*, q_3^*, q_4^*)\\
&\quad + f_1(l_{01}, q_1^*, q_2^*, q_3^*, q_4^*)(x_a^d - \gamma_1),
\end{aligned} \tag{36}$$

where

$$\begin{aligned}
f_0(x_r, l_{01}, q_1^*, q_2^*, q_3^*, q_4^*) &= A + B\big(x_r - \hat{m}_{pp}^{-1} C\big),\\
f_1(l_{01}, q_1^*, q_2^*, q_3^*, q_4^*) &= D - B\hat{m}_{pp}^{-1} E,
\end{aligned}$$

with matrices A, B, C, D, and E expressed in Appendix B.

Considering estimate (36), system (32) can be approximated by the following affine system in strict feedback form with perturbation terms:

$$\begin{aligned}
\dot{z}_1 &= \dot{x}_r^d - \hat{m}_{pp}^{-1}(l_{01}, q_1^*, q_2^*, q_3^*, q_4^*)\big(y_r^d - z_2\big) - \varepsilon_1,\\
\dot{z}_2 &= \dot{y}_r^d - f_0(x_r, l_{01}, q_1^*, q_2^*, q_3^*, q_4^*)\\
&\quad - f_1(l_{01}, q_1^*, q_2^*, q_3^*, q_4^*) \times \big(x_a^d - \gamma_1\big) - \varepsilon_3,\\
\dot{\gamma}_1 &= \gamma_2,\\
\dot{\gamma}_2 &= \dot{y}_a^d - u,
\end{aligned} \tag{37}$$

where $\varepsilon_3 = \varepsilon_2 + f_r - \hat{f}_r$. Despite the fact that the approximate system (37) introduces an additional modeling error $f_r - \hat{f}_r$, the following lemma ensures that the perturbation terms are bounded.

Lemma 1. Boundedness of the perturbed terms: The perturbation terms ε_1 and ε_3 in the quadruped robot dynamics (37) are bounded, i.e., there exist positive constants $\delta_i > 0, i = 1, 2$ such that $\|\varepsilon_1\| \le \delta_1$ and $\|\varepsilon_3\| \le \delta_2$ are satisfied.

Proof. The quadruped robot model is a periodic motion system, and thus, the generalized coordinate velocities, accelerations, and momentum $(x, \dot{x}, \ddot{x}$, and $y_r)$ are all bounded. Then, all perturbation terms in Eq. (37) are bounded, and one has $\delta_1 \ge \max(\|\varepsilon_1\|)$, $\delta_2 \ge \max(\|\varepsilon_3\|)$. □

For the purpose of clarity and simplicity, Eq. (37) can be rewritten in a more compact form as

$$\begin{aligned}
\dot{z}_1 &= h_1(t) + g_1 z_2 - \varepsilon_1,\\
\dot{z}_2 &= h_2(t) + B z_1 + f_1 \gamma_1 - \varepsilon_3,\\
\dot{\gamma}_1 &= \gamma_2,\\
\dot{\gamma}_2 &= h_3(t) - u,
\end{aligned} \tag{38}$$

where $h_1(t) = \dot{x}_r^d - \hat{m}_{pp}^{-1} y_r^d$, $h_2(t) = \dot{y}_r^d - A - B x_r^d + B\hat{m}_{pp}^{-1} C - f_1 x_a^d$, and $g_1 = \hat{m}_{pp}^{-1}$.

https://doi.org/10.1017/S0263574712000458 Published online by Cambridge University Press

The main result of the paper is presented in the following theorem which offers a method for the stabilization and control of the five-link model of quadruped robot in bounding motion.

Theorem. Robust backstepping control of quadruped robot model in bounding motion: Consider system (38) and arbitrary scalar constants $k_1, k_2, k_3, k_4 > 0$, $\eta_1, \eta_2 > 0$, and assume that the upper bounds $\delta_1 \geq \max(\|\varepsilon_1\|)$, $\delta_2 \geq \max(\|\varepsilon_3\|)$ are known. Consider the smooth state feedback $u$given by

$$u = k_4 e_{\gamma_2} + \left(\frac{\partial H_3}{\partial \gamma_1}\right)^T + h_3 - \frac{\partial(\lambda_3)}{\partial \gamma_1}(\gamma_2) - \frac{\partial(\lambda_3)}{\partial z_2}(h_2 + Bz_1 + f_1\gamma_1) - \frac{\partial(\lambda_3)}{\partial z_1}(h_1 + g_1 z_2), \tag{39}$$

where positive definite functions $H_i(\cdot)$ are

$$H_1(z_1) = \frac{1}{2} z_1^T z_1,$$

$$H_2(z_1, z_2) = \frac{1}{2} z_1^T z_1 + \frac{1}{2}(z_2 - \lambda_1)^T (z_2 - \lambda_1),$$

$$H_3(z_1, z_2, \gamma_1) = H_2(z_1, z_2) + \frac{1}{2}(\gamma_1 - \lambda_2)^T (\gamma_1 - \lambda_2), \tag{40}$$

$$H_4(z_1, z_2, \gamma_1, \gamma_2) = H_3(z_1, z_2, \gamma_1) + \frac{1}{2}(\gamma_2 - \lambda_3)^T (\gamma_2 - \lambda_3),$$

and

$$\lambda_3(z_1, z_2, \gamma_1) = -k_3 e_{\gamma_1} - \left(\frac{\partial H_2}{\partial z_2} f_1\right)^T + \frac{\partial \lambda_2}{\partial z_2}(h_2 + Bz_1 + f_1\gamma_1) + \frac{\partial \lambda_2}{\partial z_1}(h_1 + g_1\gamma_2),$$

$$f_1\lambda_2(z_1, z_2) = -\left(k_2 + \eta_2\delta_2^2\right)(z_2 - \lambda_1) - \left(\frac{\partial H_1}{\partial z_1} g_1\right)^T - h_2 - Bz_1 + \frac{\partial \lambda_1}{\partial z_1}(h_1 + g_1 z_2),$$

$$g_1\lambda_1(z_1) = -(k_1 + \eta_1\delta_1^2)z_1 - h_1.$$

Then, the control law (39) guarantees system (37) to become uniformly bounded, i.e., there exists a positive constant σ such that the state vector converges to the following compact residual set:

$$\Omega = \{(z_1, z_2, \gamma_1, \gamma_2) : H(z, \gamma) \leq \sigma\}, \tag{41}$$

where $H(z, \gamma) = H_4(z_1, z_2, \gamma_1, \gamma_2)$.

Proof. Consider the $z_1$subsystem of Eq. (37), select $H_1(z_1)$ as the candidate Lyapanov function and view z_2 as the virtual input for z_1 subsystem, then using inequalities: $2ab \leq a^2 + b^2$ and $\left|a^T b\right| \leq \|a\| . \|b\|$, for every $\eta_1 > 0$ one can write

$$\begin{aligned}\dot{H}_1(z_1) &= z_1^T \dot{z}_1 \\ &= z_1^T \left[h_1 + g_1 z_2 - \varepsilon_1\right] \leq z_1^T \left[h_1 + g_1 z_2\right] \\ &\quad + \eta_1 \left\|z_1^T\right\|^2 \|\varepsilon_1\|^2 + 1/(4\eta_1) \\ &\leq z_1^T\left[h_1 + g_1 z_2 + \eta_1\delta_1^2 z_1\right] + 1/(4\eta_1).\end{aligned} \tag{42}$$

Let $g_1 z_2 = -(k_1 + \eta_1\delta_1^2)z_1 - h_1$, where $k_1 > 0$ is arbitrary, then Eq. (42) reduces to

$$\dot{H}_1(z_1) \leq -k_1 z_1^T z_1 + 1/(4\eta_1). \tag{43}$$

Furthermore, select $H_2(z_1, z_2)$ as the candidate Lyapanov function for composite subsystem (z_1, z_2), with γ_1 as its virtual input and let $e_{z_2} = z_2 - \lambda_1(z_1)$, then it follows that:

$$\begin{aligned}\dot{H}_2(z_1, z_2) &= \dot{H}_1(z_1) + e_{z_2}^T(\dot{z}_2 - \dot{\lambda}_1(z_1)) \\ &= \frac{\partial H_1}{\partial z_1}\left[h_1 + g_1(e_{z_2} + \lambda_1) - \varepsilon_1\right] \\ &\quad + e_{z_2}^T\left[h_2 + Bz_1 + f_1\gamma_1 - \varepsilon_3 - \frac{\partial \lambda_1}{\partial z_1}(h_1 + g_1 z_2)\right] \\ &= \frac{\partial H_1}{\partial z_1}\left[h_1 + g_1\lambda_1 - \varepsilon_1\right] \\ &\quad + e_{z_2}^T\left[\left(\frac{\partial H_1}{\partial z_1} g_1\right)^T + h_2 + Bz_1 + f_1\gamma_1 - \varepsilon_3 \right. \\ &\quad \left. - \frac{\partial \lambda_1}{\partial z_1}(h_1 + g_1 z_2)\right].\end{aligned} \tag{44}$$

Considering the inequality (43), Eq. (44) yields

$$\begin{aligned}\dot{H}_2(z_1, z_2) &\leq -k_1 z_1^T z_1 + e_{z_2}^T\left[\left(\frac{\partial H_1}{\partial z_1} g_1\right)^T + h_2 + Bz_1 \right. \\ &\quad \left. + f_1\gamma_1 - \varepsilon_3 - \frac{\partial \lambda_1}{\partial z_1}(h_1 + g_1 z_2)\right] + \frac{1}{4\eta_1} \\ &\leq -k_1 z_1^T z_1 + e_{z_2}^T\left[\left(\frac{\partial H_1}{\partial z_1} g_1\right)^T + h_2 + Bz_1 + f_1\lambda_2 \right. \\ &\quad \left. + f_1(\gamma_1 - \lambda_2) - \frac{\partial \lambda_1}{\partial z_1}(h_1 + g_1 z_2) + \eta_2\delta_2^2 e_{z_2}\right] + \xi\ ,\end{aligned} \tag{45}$$

where $\xi = 1/(4\eta_1) + 1/(4\eta_2)$. Let

$$f_1\lambda_2 = -(k_2 + \eta_2\delta_2^2)e_{z_2} - \left(\frac{\partial H_1}{\partial z_1} g_1\right)^T - h_2 - Bz_1 + \frac{\partial \lambda_1}{\partial z_1}(h_1 + g_1 z_2),$$

where $k_2 > 0$ is arbitrary. From the inequality (45), one can write

$$\dot{H}_2(z_1, z_2) \leq -k_1 z_1^T z_1 - k_2 e_{z_2}^T e_{z_2} + \frac{\partial H_2}{\partial Z_2} f_1(\gamma_1 - \lambda_2) + \xi. \tag{46}$$

Furthermore, select $H_3(z_1, z_2, \gamma_1)$ as the candidate Lyapunov function for composite subsystem (z_1, z_2, γ_1), with

https://doi.org/10.1017/S0263574712000458 Published online by Cambridge University Press

γ_2 as its new virtual input, and let $e_{\gamma_1} = \gamma_1 - \lambda_2$, then

$$\begin{aligned}\dot{H}_3(z_1, z_2, \gamma_1) &= \dot{H}_2(z_1, z_2) + e_{\gamma_1}^T(\dot{\gamma}_1 - \dot{\lambda}_2)\\ &\le -k_1 z_1^T z_1 - k_2 e_{z_2}^T e_{z_2} + e_{\gamma_1}^T\Bigg[\left(\frac{\partial H_2}{\partial z_2} f_1\right)^T\\ &\quad +\lambda_3 + (\gamma_2 - \lambda_3) - \frac{\partial \lambda_2}{\partial z_2}(h_2 + B z_1 + f_1\gamma_1)\\ &\quad - \frac{\partial \lambda_2}{\partial z_1}(h_1 + g_1\gamma_2)\Bigg] + \xi.\end{aligned} \tag{47}$$

Letting

$$\lambda_3(z_1, z_2, \gamma_1) = -k_3 e_{\gamma_1} - \left(\frac{\partial H_2}{\partial z_2} f_1\right)^T + \frac{\partial \lambda_2}{\partial z_2}(h_2 + B z_1 + f_1\gamma_1) + \frac{\partial \lambda_2}{\partial z_1}(h_1 + g_1\gamma_2),$$

with arbitrary $k_3 > 0$, inequality (47) reduces to

$$\begin{aligned}\dot{H}_3(z_1, z_2, \gamma_1) &\le \dot{H}_2(z_1, z_2) - k_3 e_{\gamma_1}^T e_{\gamma_1} + e_{\lambda_1}^T(\gamma_2 - \lambda_3) + \xi\\ &= -k_1 z_1^T z_1 - k_2 e_{z_2}^T e_{z_2} - k_3 e_{\gamma_1}^T e_{\gamma_1}\\ &\quad + \frac{\partial H_3}{\partial \gamma_1}(\gamma_2 - \lambda_3) + \xi.\end{aligned} \tag{48}$$

Finally, selecting $H_4(z_1, z_2, \gamma_1, \gamma_2)$ as the candidate Lyapunov function for the system (38), and letting $e_{\gamma_2} = \gamma_2 - \lambda_3$ follows that:

$$\begin{aligned}\dot{H}_4(z_1, z_2, \gamma_1, \gamma_2) &= \dot{H}_3(z_1, z_2, \gamma_1) + e_{\gamma_2}^T(\dot{\gamma}_2 - \dot{\lambda}_3)\\ &\le -k_1 z_1^T z_1 - k_2 e_{z_2}^T e_{z_2} - k_3 e_{\gamma_1}^T e_{\gamma_1}\\ &\quad + e_{\gamma_2}^T\Bigg[\left(\frac{\partial H_3}{\partial \gamma_1}\right)^T + h_3 - u\\ &\quad - \frac{\partial \lambda_3}{\partial \gamma_1}(\gamma_2) - \frac{\partial \lambda_3}{\partial z_2}(h_2 + B z_1 + f_1\gamma_1)\\ &\quad - \frac{\partial \lambda_3}{\partial z_1}(h_1 + g_1 z_2)\Bigg] + \xi.\end{aligned} \tag{49}$$

With

$$u = k_4 e_{\gamma_2} + \left(\frac{\partial H_3}{\partial \gamma_1}\right)^T + h_3 - \frac{\partial \lambda_3}{\partial \gamma_1}(\gamma_2) - \frac{\partial \lambda_3}{\partial z_2}(h_2 + B z_1 + f_1\gamma_1) - \frac{\partial \lambda_3}{\partial z_1}(h_1 + g_1 z_2), \tag{50}$$

as the actual input for the system (38) in which $k_4 > 0$ is arbitrary, inequality (49) follows:

$$\dot{H}_4(z_1, z_2, \gamma_1, \gamma_2) \le -k_1 z_1^T z_1 - k_2 e_{z_2}^T e_{z_2} - k_3 e_{\gamma_1}^T e_{\gamma_1} - k_4 e_{\gamma_2}^T e_{\gamma_2} + \xi. \tag{51}$$

For simplicity, let $k_1 = k_2 = k_3 = k_4 = 0.5\,\rho > 0$. Then, inequality (51) is rewritten as

$$\dot{H}_4 \le -\rho H_4 + \xi. \tag{52}$$

Table I. The physical parameters of the Little-Dog.[3].

Symbol	Value	Unit	Description
Shin			
$\Delta l_{0\max}$	4.5	cm	Maximum spring travel
K	7500	N/m	Spring linear stiffness
m_1	0.13	kg	Mass of shin
l_1	9.2	cm	Length of shin (rigid part)
I_1	7×10^{-5}	Kg.m^2	Inertia of shin
r_1	5.7	cm	Center of mass
Upper leg			
m_2	0.24	kg	Mass of upper leg
l_2	7.5	cm	Length of upper leg
I_2	6×10^{-6}	Kg.m^2	Inertia of upper leg
r_2	4.8	cm	Center of mass
Body			
m_3	2.3	kg	Mass of body
l_3	20.2	cm	Length of body
I_3	2.2×10^{-3}	Kg.m^2	Inertia of body
r_3	8.7	cm	Center of mass

Thus

$$\begin{aligned}H_4(t) &\le H_4(t_0)e^{-\rho(t-t_0)} + (\xi/\rho)(1 - e^{-\rho(t-t_0)})\\ &\le H_4(t_0)e^{-\rho(t-t_0)} + (\xi/\rho).\end{aligned} \tag{53}$$

From Eq. (40), it is clear that $H_4(t) \ge \max\{\frac{1}{2}z_1^T z_1, \frac{1}{2}e_{z_2}^T e_{z_2}, \frac{1}{2}e_{\gamma_1}^T e_{\gamma_1}, \frac{1}{2}e_{\gamma_2}^T e_{\gamma_2}\}$. Moreover, it is trivial that $\lim_{t\to\infty} H_4(t_0)e^{-\rho(t-t_0)} = 0$. Therefore, for all $\rho > 0$there exists a constant $\xi_0 > 0$ such that

$$H_4(t_0)e^{-\rho(t-t_0)} < \xi_0,\ t > T.$$

Hence, we have

$$\|\chi_i\| < 2(\xi_0 + \xi/\rho), \qquad i = 1, 2, 3, 4, \tag{54}$$

where$\chi_1 = z_1, \chi_2 = e_{z_2}, \chi_3 = e_{\gamma_1}, \chi_4 = e_{\gamma_2}$. By selecting the independent parameters ρ, η_1, η_2, there exists a σ such that

$$H_4(z_1, z_2, \gamma_1, \gamma_2) \le \sigma \le \xi_0/\rho. \tag{55}$$

This completes the proof. □

Remark 4: The proposed robust backstepping control (39) depends on the bound of perturbation terms of system (38). With the periodic motion manner of the quadruped robot in bounding motion, the perturbations in the system (38) are bounded in principle.

5. Numerical Simulation

The control aim is that the hand of the quadruped robot tracks a desired path and the robot does a complete bounding step motion, which will be helpful for different tasks such as passing an obstacle. We would like to test the robustness of the proposed controller in the presence of model uncertainties. For simulating the quadruped robot, we use the physical parameters of the Little-Dog[3] which are given in Table I.

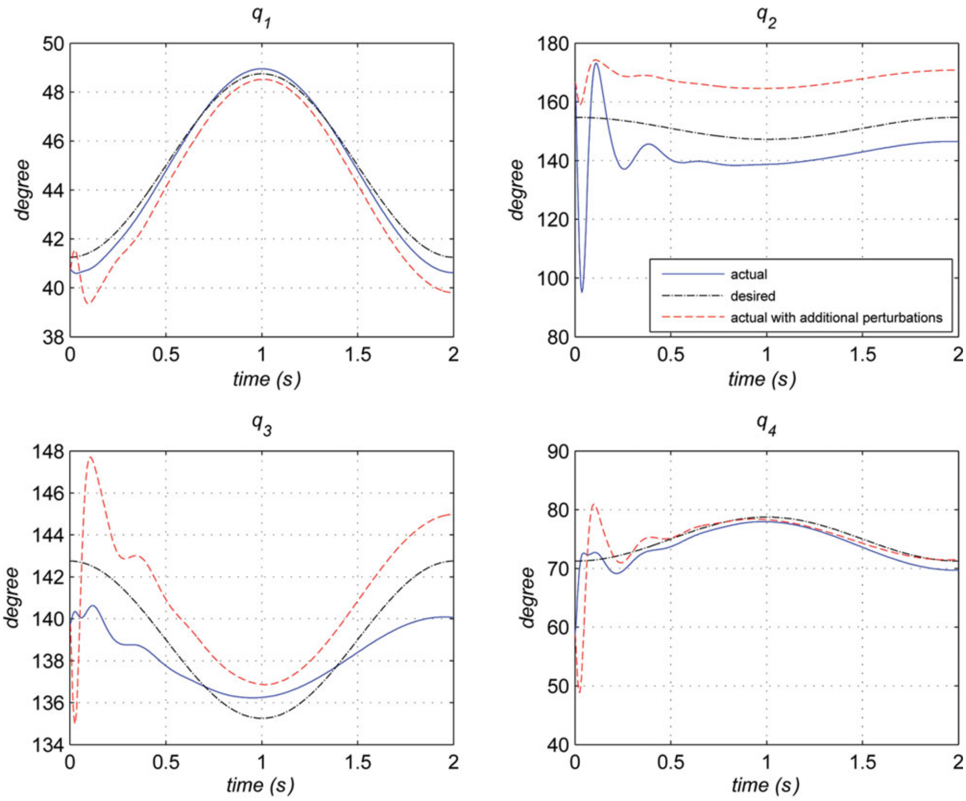

Fig. 3. (Colour online) The active joints of the closed-loop system in bounding motion.

For bounding motion, the actuators situated in the joints should follow a certain path. Thus, a path planning is needed. However, with simple calculations, we can assign a path for every joint so that the bounding is realized. Particularly, we choose the following path for each joint:

$$x_i^d(t) = \alpha + \beta \sin(\omega t + \kappa), \; i = 1, \ldots, 6, \tag{56}$$

where α, β, ω, and κ are the parameters selected to have proper robot bounding gesture and x_i $(i = 1, \ldots, 6)$ are $\varphi, l_0, q_1, q_2, q_3, q_4$, respectively (see Fig. 2). The nominal operating points of the paths are obtained by

$$x_i^* = \frac{1}{2}\left(x_i^{\min} + x_i^{\max}\right), \tag{57}$$

where $x_i^{\min}$, $x_i^{\max}$ are the minimum and maximum values of the selected paths given in Eq. (56). Table II shows the choice of these parameters as well as the minimum, maximum, and the nominal operating points of these paths.

Using the robust controller (39) and the desired path (56), we simulate the dynamic Eq. (38) with MATLAB. At first, the desired path is transformed to the form given in Eq. (14); then the model and the controller are implemented. Afterwards, by utilizing coordinate transformation (14), the active and passive variables appear.

The designed controller is robust as it tackles unstructured uncertainties of the approximate model. In addition, we add parameter variations (as additional uncertainties) to the simulations. On the other hand, our controller is a model-based controller, and thus the parameter uncertainties must also be tested. These uncertainties can be the result of measurement errors or possible changes in the model. Therefore, we randomly change all the mass parameters of the model indicated in Table I between 1 and 15% and compare the results of simulations with and without uncertainties.

Table II. Values of the selected paths..

(x_i^d)	Minimum $(x_i^{\min})$	Maximum $(x_i^{\max})$	Operation point (x_i^*)
l_0 (cm)	1.95	3.6	2.8
φ (degree)	116	134	125
q_1 (degree)	41.5	48.5	45
q_2 (degree)	148	155	151.5
q_3 (degree)	135	142.5	138.75
q_4 (degree)	70	79	74.5

Figure 3 shows the angular displacement of the active joints of the planar model, which indicates that the four active joints of the robot follow the determined path with a small overshoot. The dot-dashed green lines indicate the desired path, the blue lines refer the results of the actual closed-loop system design based on the nominal parameters of the original nonlinear system, and the dashed red lines refer to results of the system with additional parameter perturbations (due to 1 15% change in mass parameters). The passive joint angle φ and passive spring length l_0 of the robot leg are shown in Fig. 4. The passive angle φ follows the trend of other joints

https://doi.org/10.1017/S0263574712000458 Published online by Cambridge University Press

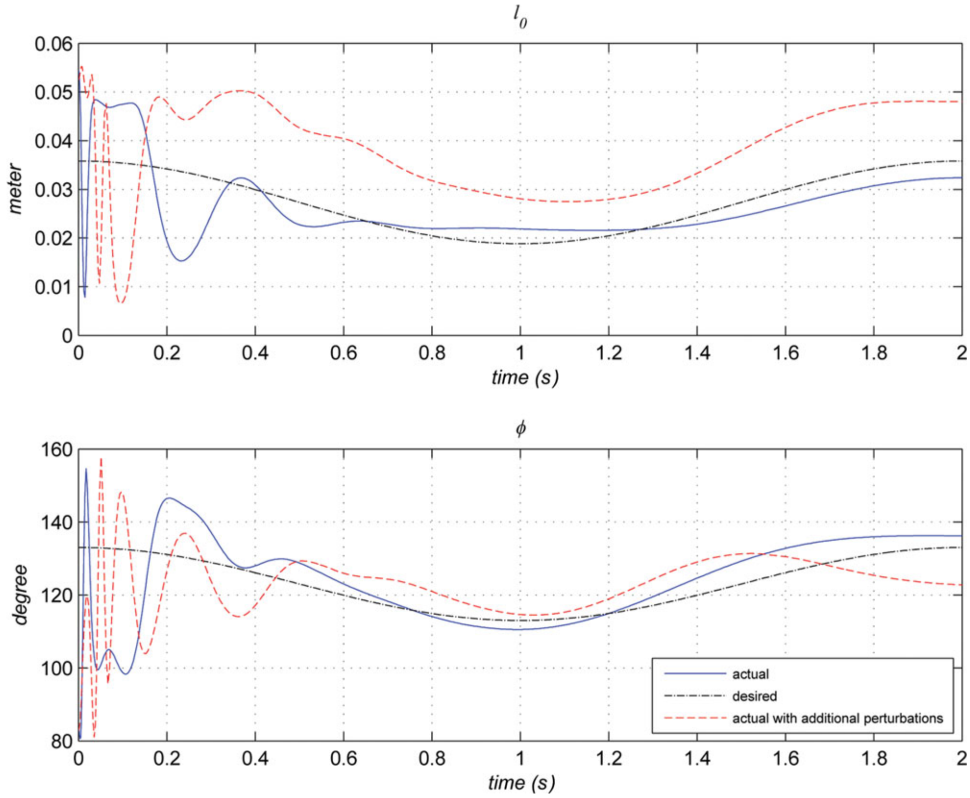

Fig. 4. (Colour online) The passive joints (l_0, φ) of the closed-loop system in bounding motion.

with a larger overshoot. The spring length has changed from its initial value to a value less than its free state value.

Figures 5 and 6 illustrate the displacements of the centers of masses of the robot links one to four. These centers of mass relate to robot's body parts shown in Fig. 2. For instance, cm_1 is related to the part with length l_1 and so on. Figure 7 shows the displacement of the end-effector of the quadruped model hand which is the tip of the last link. Figure 8 illustrates the required torques for this displacement for the bounding motion. As it is expected, by the increase in the mass of each actuator from joint 1 to joint 4 the required torque increases, but the stability of the robot is maintained. LittleDog is a small robot and thus the required torque for its movements is not high. The steady state torque is also shown in Fig. 8. Finally, in Fig. 9 the phase trajectories of variables are depicted which are obtained in periodic mode in 100 s without uncertainty which show all the states remain stable.

Finally, we would like to compare the results of our method with those of previous works. It should be noted that although there are some works on the gaiting of quadruped bounding motion,[20,21] these works do address the control of the robot dynamics. However, there exist some methods for control of underactuated manipulators[22–24] which can be used for bounding. A common method is the separation of control procedure for active and passive joints.[22–24] Although such method is only proper for convergence to a position not trajectory, ref. [22] uses the sliding mode method to control the active joints as a fully actuated system by choosing fixed values for the passive joints. To compare our method with the method presented in ref. [22], we employ it for bounding motion of quadruped robot model by defining sliding surface and control as

$$s = \Gamma_a(x_a^d - x_a) + \dot{x}_a^d - \dot{x}_a \quad \text{and}$$
$$u = \Gamma_a(\dot{x}_a^d - \dot{x}_a) + \ddot{x}_a^d + p_a \mathrm{sgn}(s), \tag{58}$$

where Γ_a and p_a are positive gains. This control method is applied to Eq. (8) supposing that the passive joints are fixed, i.e., $l_o = 2.8$ cm and $\varphi = 120°$. Figure 10 shows the result of this simulation. As we can see from the figure, the displacement of the robot with the sliding mode control is not efficient in comparison with that of results with backstepping method. This is expected since the passive joints are fixed and are not controlled in the sliding mode method given in ref. [22].

6. Conclusions

In this paper, the control of an underactuated quadruped robot in bounding state was discussed. Considering the complexities of the quadruped robot, a simplified quadruped model with six DOF involving four actuated and two unactuated joints was presented. Next, the dynamical equations of this model were obtained which are second-order nonholonomic equations. The resulting highly nonlinear model was transformed to a strict feedback form. This transformation is suitable for other mechanical systems with the same number of actuated and unactuated variables as well. The transformation simplifies the dynamical equations of the system since the control variable appears only in the last subsystem. The transformation has perturbed terms due

https://doi.org/10.1017/S0263574712000458 Published online by Cambridge University Press

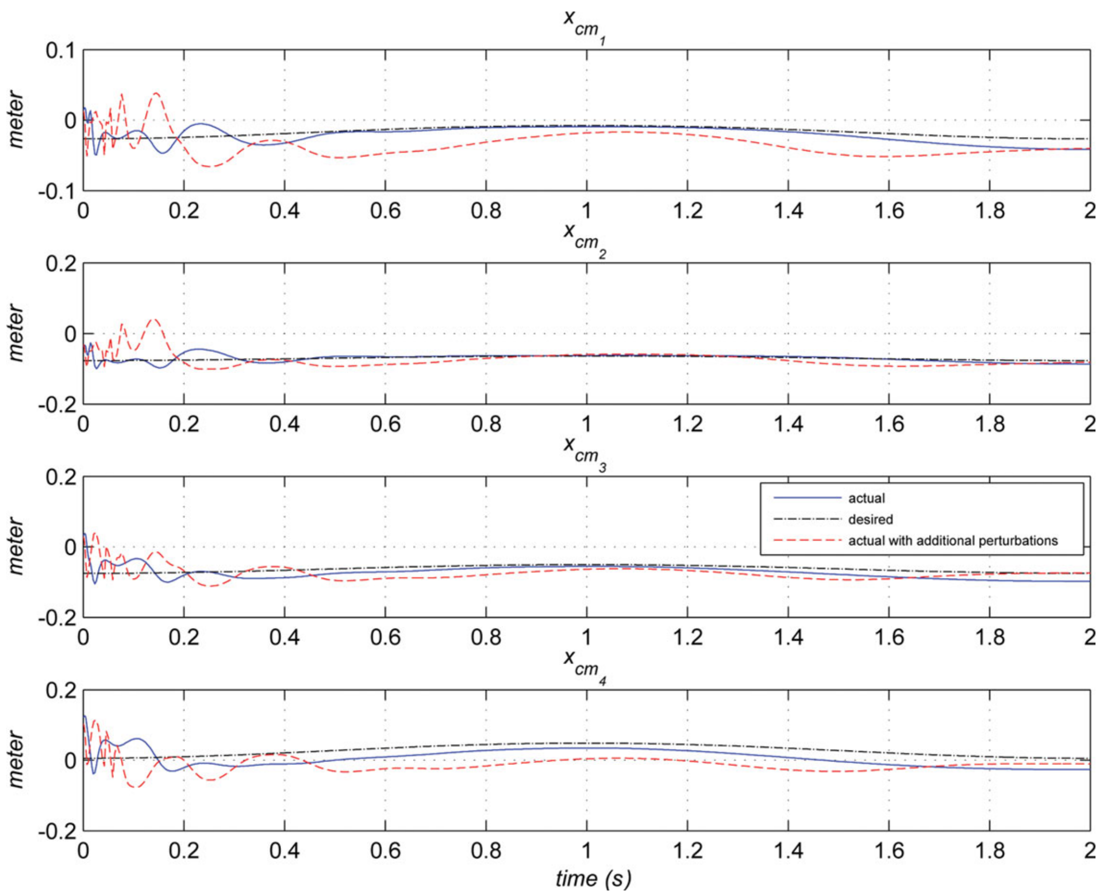

Fig. 5. (Colour online) Displacements of the centers of masses of the robot links (x-axis).

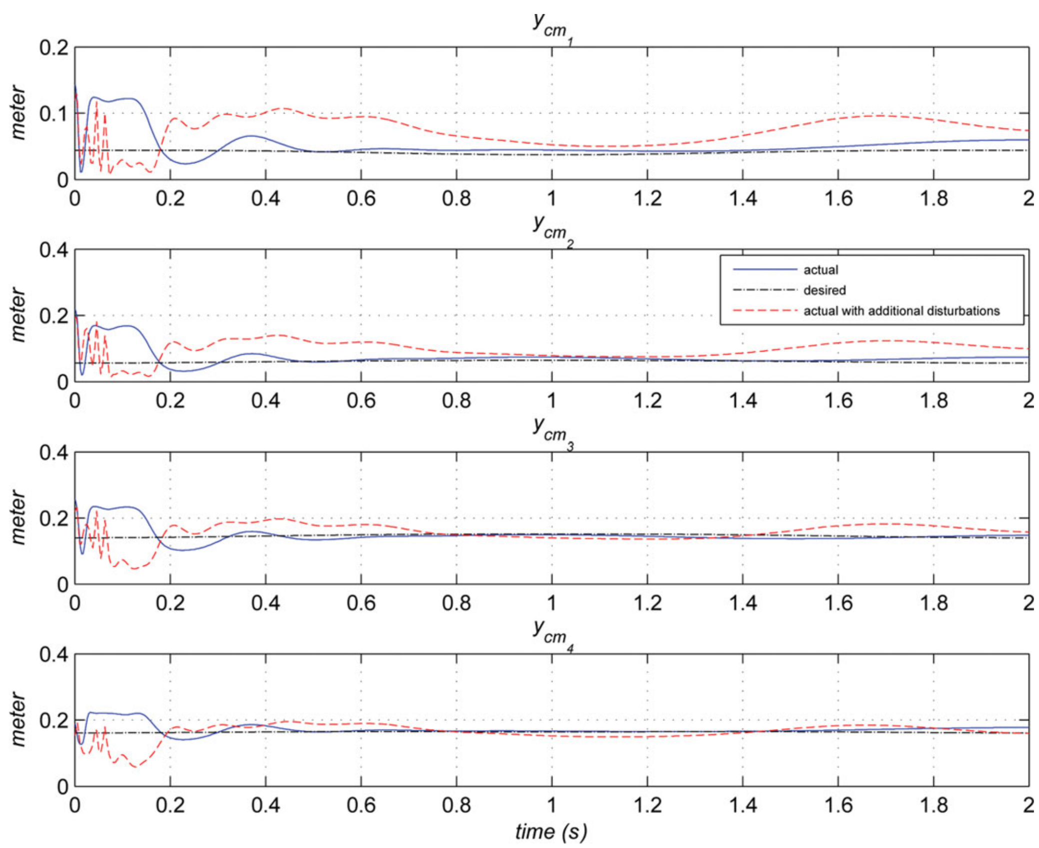

Fig. 6. (Colour online) Displacements of the centers of masses of the robot links (y-axis).

https://doi.org/10.1017/S0263574712000458 Published online by Cambridge University Press

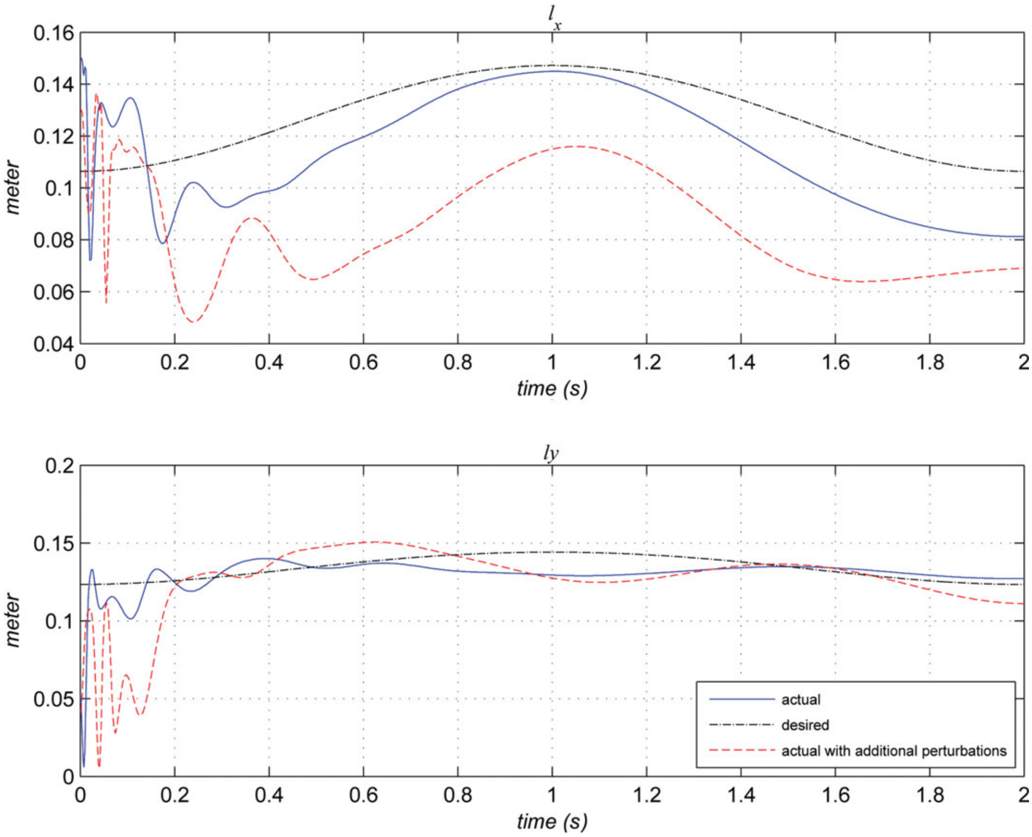

Fig. 7. (Colour online) Displacement of the robot's hand.

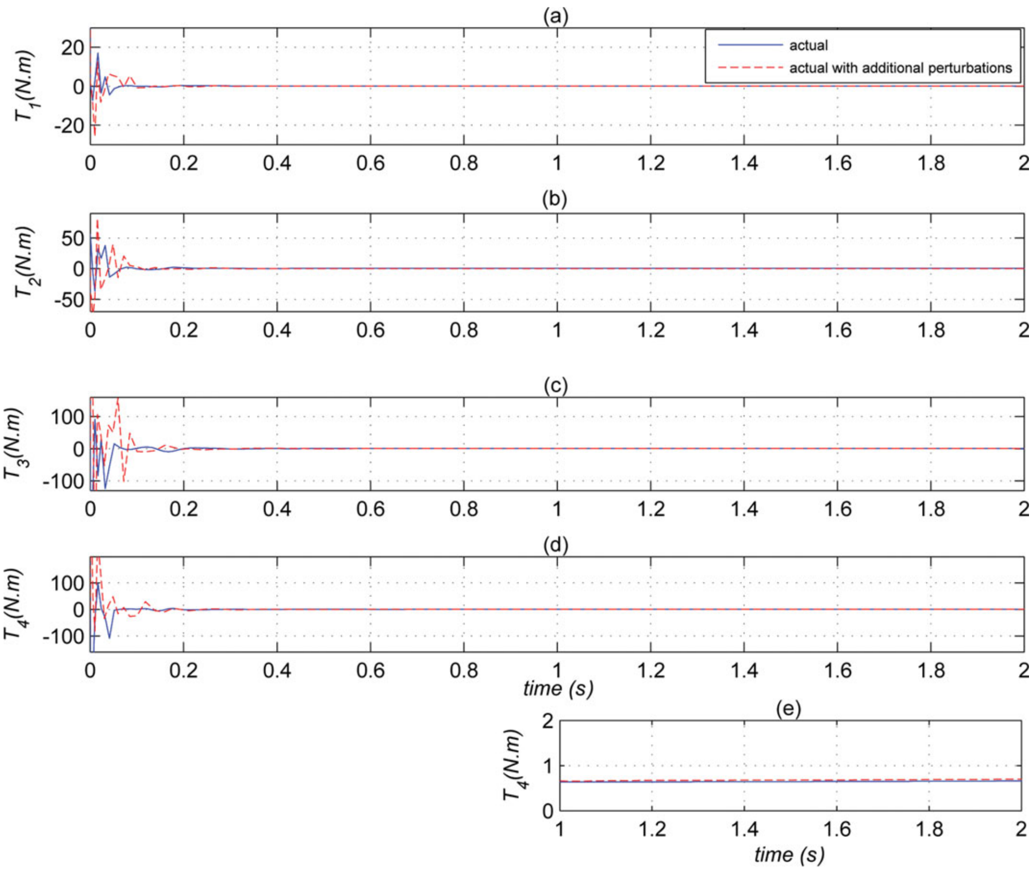

Fig. 8. (Colour online) (a)–(d) The torques of the actuators, (e) the blow up of the fourth torque to show its steady state value.

https://doi.org/10.1017/S0263574712000458 Published online by Cambridge University Press

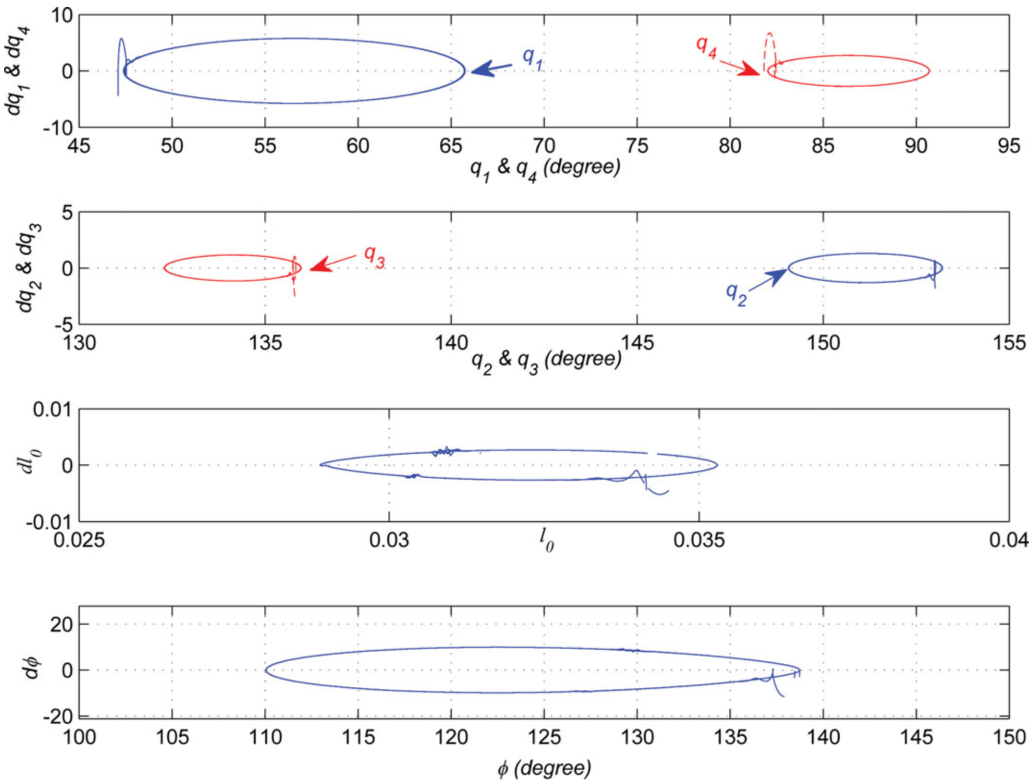

Fig. 9. (Colour online) The phase trajectories.

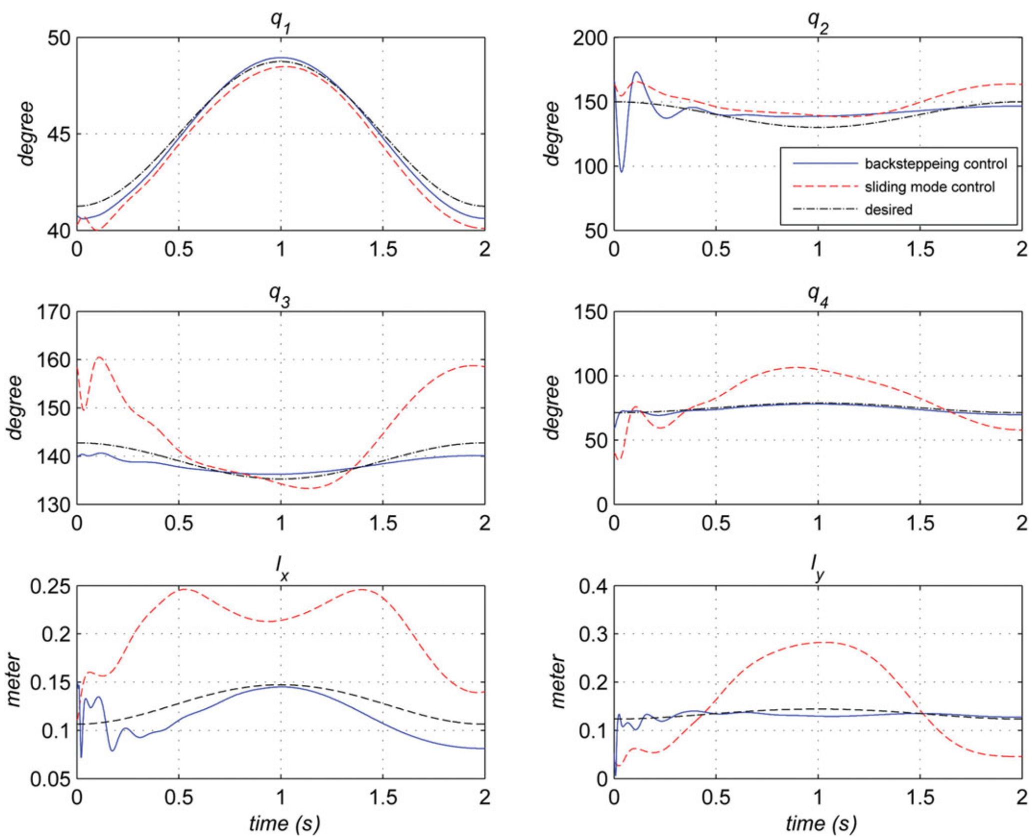

Fig. 10. (Colour online) The comparison results of the proposed backstepping method with those of the sliding mode method.

https://doi.org/10.1017/S0263574712000458 Published online by Cambridge University Press

to the estimations employed. Then, a robust backstepping feedback controller was designed, which guarantees the boundedness and convergence of the robot states. The simulation results indicate the proper behavior of the closed-loop system even when the mass parameters of the robot are perturbed by 15% of the nominal design values.

Acknowledgments

The authors would like to thank Mr. Moosa Daryanavard, Reza Oftadeh, and Navid Rahbari Asr for their useful suggestions.

References

1. R. Samperio, H. Hu, F. Martín and V. Matelln, "A hybrid approach to fast and accurate localization for legged robots," *Robotica* **26**, 817–830 (2008).
2. M. F. Silvaa1 and J. T. Machadoa, "Kinematic and dynamic performance analysis of artificial legged systems," *Robotica* **26**, 19–33 (2008).
3. A. Shkolnik, M. Levashov, I. R. Manchester and R. Tedrake, "Bounding on rough terrain with the LittleDog robot," *Int. J. Robot. Res.* **30**(3), 265–279 (2010).
4. A. Isidori, *Nonlinear Control Systems* (Springer-Verlag, Berlin, 1995).
5. Y. Hu, G. Yana and Z. Lina, "Stable running of a planar underactuated biped robot," *Robotica* **29**, 265–279 (2010).
6. K. D. Do, Z. P. Jiang and J. Pan, "Universal controllers for stabilization and tracking of under-actuated ships," *Syst. Control Lett.* **47**, 299–317 (2002).
7. A. D. Luca, R. Mattone and G. Oriolo, "Stabilization of an under-actuated planar 2R manipulator," *Int. J. Robust Nonlinear Control* **10**, 181–198 (2000).
8. A. D. Luca and G. Oriolo, "Trajectory planning and control for planar robots with passive last joint," *Int. J. Robust Nonlinear Control* **21**(5–6), 575–590 (2002).
9. R. M. Murray, Zexiang Li and S. Shankar Sastry, *A Mathematical Introduction to Robotics Manipulation* (CRC Press, Boca Raton, FL, 1994).
10. R. Olfati-Saber, Nonlinear Control of Underactuated Mechanical Systems with Application to Robotics and Aerospace Vehicles, *Doctoral Dissertation* (Cambridge: Massachusetts Institute of Technology, 2001).
11. S. Sastry, *Nonlinear Systems Analysis, Stability and Control* (Springer-Verlag, New York, 1999).
12. F. Mazenc and L. Praly, "Adding integrations, saturated controls and stabilization for feedforward systems," *IEEE Trans. Autom. Control* **40**, 1559–1578 (1996).
13. I. Poulakakis, E. Papadopoulos and M. Buhler, "On the stability of the passive dynamics of quadrupedal running with a bounding gait," *Int. J. Robot.* **25**, 669–687 (2006).
14. R. A. Freeman and P. V. Kokotović, *Robust Nonlinear Control Design: State-Space and Lyapunov Techniques* (Birkh auser, Boston, 1996).
15. C. Samson, "Control of chained systems application to path following and time-vary point-stabilization of mobile robots," *IEEE Trans. Autom. Control* **40**(1), 64–77 (1995).
16. P. Lucibello and G. Oriolo, "Robust stabilization via iterative state steering with an application to chained-form systems," *Automatica* **37**, 71–79 (2001).
17. N. Marchand and M. Alamir, "Discontinuous exponential stabilization of chained form systems," *Automatica* **39**, 343–348 (2003).
18. H. Guangping and Z. Geng, "Robust backstepping control of an under-actuated one-legged hopping robot in stance phase," *Robotica* **28**, 583–596 (2010).
19. M. Kristić, I. Kanellakopoulos and P. Kokotović, *Nonlinearand Adaptive Control Design* (John Wiley & Sons, San Francisco, CA, 1995).
20. D. Campbell and M. Buehler, *Preliminary Bounding Experiments in a Dynamic Hexapod* (Ambulatory Robotics Lab, Centre for Intelligent Machines, McGill University, Montreal, Canada, 2002).
21. S. Talebi, I. Poulakakis, E. Papadopoulos and M. Buehler, "Quadruped Robot Running with a Bounding Gait," **In**: *Experimental Robotics VII, in Lecture notes in Control and Information Sciences* (D. Rus and S. Singh, eds.) (Springer-Verlag, Berlin 2001) vol. 271, pp. 281–289.
22. M. Bergerman, Dynamics and Control of Underactuated Manipulators, *Doctoral Dissertation* (Pennsylvania: Carnegie Mellon University, 1996).
23. W. C. Yueqing, Y. X. Zhao and Q. Sun "Position control of a 2DOF underactuated planar flexible manipulator," *Proceedings of the IEEE International Conference on Mechatronics and Automation*, Beijing, China (Aug. 7–10, 2011) pp. 464–469.
24. S. Mahjoub, F. Mnif and N. Derbel, "Set point stabilization of a 2DOF underactuated manipulator," *J. Comput.* **6**(2), 368–376 (2011).

Appendix A: The inertia matrix of quadruped robot model in bounding motion

The positions of Center of Mass (CM) of the links for the underactuated quadruped robot are given as follows:

The CM of the shin

$$\begin{cases} l_{x_{c1}} = (l_0 + l_{10})\cos(\varphi), \\ l_{y_{c1}} = (l_0 + l_{10})\sin(\varphi). \end{cases} \tag{A 1}$$

The upper leg

$$\begin{cases} l_{x_{c2}} = (l_0 + l_1)\cos(\varphi) + l_{20}\cos(\varphi + q_4), \\ l_{y_{c2}} = (l_0 + l_1)\cos(\varphi) + l_{20}\cos(\varphi + q_4). \end{cases} \tag{A 2}$$

The body

$$\begin{cases} l_{x_{c3}} = (l_0 + l_1)\cos(\varphi) + l_2\cos(\varphi + q_4) + l_{30} \\ \quad \cos(\varphi + q_4 + q_3), \\ l_{y_{c3}} = (l_0 + l_1)\sin(\varphi) + l_2\sin(\varphi + q_4) + l_{30} \\ \quad \sin(\varphi + q_4 + q_3). \end{cases} \tag{A 3}$$

The arm

$$\begin{cases} l_{x_{c4}} = (l_0 + l_1)\cos(\varphi) + l_2\cos(\varphi + q_4) + l_3 \\ \quad \cos(\varphi + q_4 + q_3) + l_{40}\cos(\varphi + q_4 + q_3 + q_2), \\ l_{y_{c4}} = (l_0 + l_1)\sin(\varphi) + l_2\sin(\varphi + q_4) + l_3 \\ \quad \sin(\varphi + q_4 + q_3) + l_{40}\sin(\varphi + q_4 + q_3 + q_2). \end{cases} \tag{A 4}$$

The hand

$$\begin{cases} l_{x_{c5}} = (l_0 + l_1)\cos(\varphi) + l_2\cos(\varphi + q_4) + l_3 \\ \quad \cos(\varphi + q_4 + q_3) + l_4\cos(\varphi + q_4 + q_3 + q_2) \\ \quad + l_5\cos(\varphi + q_4 + q_3 + q_2 + q_1), \\ l_{y_{c5}} = (l_0 + l_1)\sin(\varphi) + l_2\sin(\varphi + q_4) + l_3 \\ \quad \sin(\varphi + q_4 + q_3) + l_4\sin(\varphi + q_4 + q_3 + q_2) \\ \quad + l_5\sin(\varphi + q_4 + q_3 + q_2 + q_1). \end{cases} \tag{A 5}$$

The kinetic energy of the robot system is

$$K = K_t + K_r, \tag{A 6}$$

where

$$K_t = \frac{1}{2}\big[m_1(\dot{l}_{xc1}^2 + \dot{l}_{yc1}^2) + m_2(\dot{l}_{xc2}^2 + \dot{l}_{yc2}^2) + m_3(\dot{l}_{xc3}^2 + \dot{l}_{yc3}^2) + m_4(\dot{l}_{xc4}^2 + \dot{l}_{yc4}^2) + m_5(\dot{l}_{xc5}^2 + \dot{l}_{yc5}^2)\big],$$

https://doi.org/10.1017/S0263574712000458 Published online by Cambridge University Press

$$K_r = \frac{1}{2}\left[I_1\dot{\varphi}^2 + I_2(\dot{\varphi}^2 + \dot{q}_4^2) + I_3(\dot{\varphi}^2 + \dot{q}_3^2 + \dot{q}_4^2) + I_4(\dot{\varphi}^2 + \dot{q}_2^2 + \dot{q}_3^2 + \dot{q}_4^2)\right.$$
$$\left. + I_5(\dot{\varphi}^2 + \dot{q}_1^2 + \dot{q}_2^2 + \dot{q}_3^2 + \dot{q}_4^2\right].$$

The potential energy of the robot is

$$V = m_1 g l_{yc1} + m_2 g l_{yc2} + m_3 g l_{yc3} + m_4 g l_{yc4} + m_5 g l_{yc5} + 1/2k(\Delta l_0)^2, \tag{A 7}$$

where k is the stiffness of the spring and g is the gravitational acceleration. Let $x = [l_0, \varphi, q_1, q_2, q_3, q_4]^T$, then the kinetic energy has form

$$K = \frac{1}{2}\dot{x}^T M(x)\dot{x}, \tag{A 8}$$

where

$$M(x) = \begin{bmatrix} m_{pp} & m_{pa} \\ m_{ap} & m_{aa} \end{bmatrix} \quad m_{pp} = \begin{bmatrix} M_{11} & M_{12} \\ M_{21} & M_{22} \end{bmatrix} \quad m_{pa} = m_{ap}^T = \begin{bmatrix} M_{13} & M_{14} & M_{15} & M_{16} \\ M_{23} & M_{24} & M_{25} & M_{26} \end{bmatrix}$$
$$m_{aa} = \begin{bmatrix} M_{33} & M_{34} & M_{35} & M_{36} \\ M_{43} & M_{44} & M_{45} & M_{46} \\ M_{53} & M_{54} & M_{55} & M_{56} \\ M_{63} & M_{64} & M_{65} & M_{66} \end{bmatrix},$$

where

$$M_{11} = m_1 + m_2 + m_3 + m_4 + m_5,$$
$$M_{12} = M_{21} = -(l_{20}m_2 + l_2(m_3 + m_4 + m_5))\sin(q_4) - (l_{30}m_3 + l_3(m_4 + m_5))\sin(q_3 + q_4)$$
$$- (l_{40}m_4 + l_4m_5)\sin(q_2 + q_3 + q_4) - l_{50}m_5\sin(q_1 + q_2 + q_3 + q_4),$$
$$M_{13} = M_{31} = -l_{50}m_5\sin(q_1 + q_2 + q_3 + q_4),$$
$$M_{14} = M_{41} = -l_{50}m_5\sin(q_1 + q_2 + q_3 + q_4) - (l_{40}m_4 + l_4m_5)\sin(q_2 + q_3 + q_4),$$
$$M_{15} = M_{51} = -(l_{30}m_3 + l_3(m_4 + m_5))\sin(q_3 + q_4) - (l_{40}m_4 + l_4m_5)\sin(q_2 + q_3 + q_4) - l_{50}m_5\sin(q_1 + q_2 + q_3 + q_4),$$
$$M_{16} = M_{61} = -(l_{20}m_2 + l_2(m_3 + m_4 + m_5))\sin(q_4) - (l_{30}m_3 + l_3(m_4 + m_5))\sin(q_3 + q_4)$$
$$- (l_{40}m_4 + l_4m_5)\sin(q_2 + q_3 + q_4) - l_{50}m_5\sin(q_1 + q_2 + q_3 + q_4),$$
$$M_{22} = I_1 + I_2 + I_3 + I_4 + I_5 + l_0^2(m_1 + m_2 + m_3 + m_4 + m_5) + l_{10}^2m_1 + l_{20}^2m_2 + l_2^2(m_3 + m_4 + m_5) + l_{30}^2m_3$$
$$+ l_3^2(m_4 + m_5) + l_{40}^2m_4 + l_4^2m_5 + l_{50}^2m_5 + 2l_0l_1(m_1 + m_2 + m_3 + m_4 + m_5) + 2l_3(l_{40}m_4 + l_4m_5)\cos(q_2)$$
$$+ 2(l_0(l_{30}m_3 + l_3(m_4 + m_5)) + l_1(l_{30}m_3 + l_3(m_4 + m_5))\cos(q_3 + q_4) + 2(l_0 + l_1)(l_{20}m_2$$
$$+ l_2(m_3 + m_4 + m_5))\cos(q_4) + 2l_4l_{50}m_5\cos(q_1) + 2l_3l_{50}m_5\cos(q_1 + q_2) + 2l_2(l_{40}m_4 + l_4m_5)\cos(q_2 + q_3)$$
$$+ 2(l_0 + l_1)(l_{40}m_4 + l_4m_5)\cos(q_2 + q_3 + q_4) + 2l_2l_{50}m_5\cos(q_1 + q_2 + q_3) + 2l_2(l_{30}m_3 + l_3(m_4 + m_5))\cos(q_3)$$
$$+ 2(l_0 + l_1)l_{50}m_4\cos(q_1 + q_2 + q_3 + q_4) + 2(l_0 + l_1)l_{50}m_5\cos(q_1 + q_2 + q_3 + q_4),$$
$$M_{23} = M_{32} = I_5 + l_{50}^2m_5 + l_4l_{50}m_5\cos(q_1) + l_3l_{50}m_5\cos(q_1 + q_2) + l_2l_{50}m_5\cos(q_1 + q_2 + q_3)$$
$$+ (l_0 + l_1)l_{50}m_5\cos(q_1 + q_2 + q_3 + q_4),$$
$$M_{24} = M_{42} = I_4 + I_5 + l_{40}^2m_4 + l_4^2m_5 + l_{50}^2m_5 + 2l_4l_{50}m_5\cos(q_1) + l_3(l_{40}m_4 + l_4m_5)\cos(q_2) + l_3l_{50}m_5\cos(q_1 + q_2)$$
$$+ l_2l_{50}m_5\cos(q_1 + q_2 + q_3) + (l_0 + l_1)l_{50}m_5\cos(q_1 + q_2 + q_3 + q_4) + l_2(l_{40}m_4 + l_4m_5)\cos(q_2 + q_3)$$
$$+ (l_0 + l_1)(l_{40}m_4 + l_4m_5)\cos(q_2 + q_3 + q_4),$$

$$M_{25} = M_{52} = I_3 + I_4 + I_5 + l_{30}^2 m_3 + l_3^2(m_4 + m_5) + l_{40}^2 m_4 + l_4^2 m_5 + l_{50}^2 m_5 + 2l_4 l_{50} m_5 \cos(q_1) + 2l_3(l_{40} m_4 + l_4 m_5)\cos(q_2)$$
$$+ l_2(l_{30} m_3 + l_3(m_4 + m_5))\cos(q_3) + 2l_3 l_{50} m_5 \cos(q_1 + q_2) + l_2 l_{50} m_5 \cos(q_1 + q_2 + q_3)$$
$$+ (l_0 + l_1) l_{50} m_5 \cos(q_1 + q_2 + q_3 + q_4) + l_2(l_{40} m_4 + l_4 m_5)\cos(q_2 + q_3) + (l_0 + l_1)(l_{40} m_4 + l_4 m_5)\cos(q_2 + q_3 + q_4)$$
$$+ (l_0(l_{30} m_3 + l_3(m_4 + m_5)) + l_1(l_{30} m_3 + l_3(m_4 + m_5))\cos(q_3 + q_4),$$
$$M_{26} = M_{62} = I_2 + I_3 + I_4 + I_5 + l_{20}^2 m_2 + l_2^2(m_3 + m_4 + m_5) + l_{30}^2 m_3 + l_3^2(m_4 + m_5) + l_{40}^2 m_4 + l_4^2 m_5 + l_{50}^2 m_5$$
$$+ 2l_4 l_{50} m_5 \cos(q_1) + 2l_3(l_{40} m_4 + l_4 m_5)\cos(q_2) + 2l_2(l_{30} m_3 + l_3(m_4 + m_5))\cos(q_3)$$
$$+ (l_0 + l_1)(l_{20} m_2 + l_2(m_3 + m_4 + m_5))\cos(q_4) + 2l_3 l_{50} m_5 \cos(q_1 + q_2)$$
$$+ 2l_2 l_{50} m_5 \cos(q_1 + q_2 + q_3) + (l_0 + l_1) l_{50} m_5 \cos(q_1 + q_2 + q_3 + q_4) + 2l_2(l_{40} m_4 + l_4 m_5)\cos(q_2 + q_3)$$
$$+ (l_0 + l_1)(l_{40} m_4 + l_4 m_5)\cos(q_2 + q_3 + q_4) + (l_0(l_{30} m_3 + l_3(m_4 + m_5)) + l_1(l_{30} m_3 + l_3(m_4 + m_5))\cos(q_3 + q_4),$$
$$M_{33} = I_5 + l_{50}^2 m_5,$$
$$M_{34} = M_{43} = I_5 + l_{50}^2 m_5 + l_1 l_{50} m_5 \cos(q_1),$$
$$M_{35} = M_{53} = I_5 + l_{50}^2 m_5 + l_4 l_{50} m_5 \cos(q_1) + l_3 l_{50} m_5 \cos(q_1 + q_2),$$
$$M_{36} = M_{63} = I_5 + l_{50}^2 m_5 + l_4 l_{50} m_5 \cos(q_1) + l_3 l_{50} m_5 \cos(q_1 + q_2) + l_2 l_{50} m_5 \cos(q_1 + q_2 + q_3),$$
$$M_{44} = I_4 + I_5 + l_{40}^2 m_4 + l_4^2 m_5 + l_{50}^2 m_5 + 2l_4 l_{50} m_5 \cos(q_1),$$
$$M_{45} = M_{54} = I_4 + I_5 + l_{40}^2 m_4 + l_4^2 m_5 + l_{50}^2 m_5 + 2l_4 l_{50} m_5 \cos(q_1) + l_3(l_{40} m_4 + l_4 m_5)\cos(q_2) + l_3 l_{50} m_5 \cos(q_1 + q_2),$$
$$M_{46} = M_{64} = I_4 + I_5 + l_{40}^2 m_4 + l_4^2 m_5 + l_{50}^2 m_5 + 2l_4 l_{50} m_5 \cos(q_1) + l_3(l_{40} m_4 + l_4 m_5)\cos(q_2) + l_2(l_{30} m_3$$
$$+ l_3(m_4 + m_5))\cos(q_3) + l_3 l_{50} m_5 \cos(q_1 + q_2) + l_2 l_{50} m_5 \cos(q_1 + q_2 + q_3) + l_2(l_{40} m_4 + l_4 m_5)\cos(q_2 + q_3)$$
$$M_{55} = I_3 + I_4 + I_5 + l_{30}^2 m_3 + l_3^2(m_4 + m_5) + l_{40}^2 m_4 + l_4^2 m_5 + l_{50}^2 m_5 + 2l_4 l_{50} m_5 \cos(q_1) + 2l_3(l_{40} m_4 + l_4 m_5)\cos(q_2)$$
$$+ 2l_3 l_{50} m_5 \cos(q_1 + q_2),$$
$$M_{56} = M_{65} = I_3 + I_4 + I_5 + l_{30}^2 m_3 + l_3^2(m_4 + m_5) + l_{40}^2 m_4 + l_4^2 m_5 + l_{50}^2 m_5 + 2l_4 l_{50} m_5 \cos(q_1) + 2l_3(l_{40} m_4 + l_4 m_5)\cos(q_2)$$
$$+ 2l_2(l_{30} m_3 + l_3(m_4 + m_5))\cos(q_3) + 2l_3 l_{50} m_5 \cos(q_1 + q_2) + l_2\,(l_{40} m_4 + l_4 m_5)\cos(q_2 + q_3)$$
$$+ l_2 l_{50} m_5 \cos(q_1 + q_2 + q_3),$$
$$M_{66} = I_2 + I_3 + I_4 + I_5 + l_{20}^2 m_2 + l_2^2(m_3 + m_4 + m_5) + l_{30}^2 m_3 + l_3^2(m_4 + m_5) + l_{40}^2 m_4 + l_4^2 m_5 + l_{50}^2 m_5 + 2l_4 l_{50} m_5 \cos(q_1)$$
$$+ 2l_3(l_{40} m_4 + l_4 m_5)\cos(q_2) + l_2(l_{30} m_3 + l_3(m_4 + m_5))\cos(q_3) + 2l_3 l_{50} m_5 \cos(q_1 + q_2)$$
$$+ l_2(l_{40} m_4 + l_4 m_5)\cos(q_2 + q_3) + l_2 l_{50} m_5 \cos(q_1 + q_2 + q_3).$$

Considering above equations since M_{11} and M_{22} are nonzero, M_{pp} is invertible.

Appendix B: The approximation of function f_r

Affine approximation of function f_r for system (32) can be rewritten as

$$\hat{f}_r = f_0(x_r, l_{01}, q_1^*, q_2^*, q_3^*, q_4^*) + f_1(l_{01}, q_1^*, q_2^*, q_3^*, q_4^*)(x_a^d - \gamma_1),$$
$$f_0(x_r, l_{01}, q_1^*, q_2^*, q_3^*, q_4^*) = A + B(x_r - \hat{m}_{pp}^{-1} C),$$
$$f_1(l_{01}, q_1^*, q_2^*, q_3^*, q_4^*) = D - B\hat{m}_{pp}^{-1} E,$$

where

$$A = \begin{bmatrix} -(m_1 + m_2 + m_3 + m_4 + m_5)g + kl_{00} \\ -0.5\pi F_0 g + g[l_{20} m_2 + l_2(m_3 + m_4 + m_5)](\sin q_4^* - q_4^* \cos q_4^*) + g[l_{30} m_3 + l_3(m_4 + m_5)](\sin(q_3^* + q_4^*) \\ -(q_3^* + q_4^*)\cos(q_3^* + q_4^*)) + g[l_{40} m_4 + l_4 m_5](\sin(q_2^* + q_3^* + q_4^*) - (q_2^* + q_3^* + q_4^*)\cos(q_2^* + q_3^* + q_4^*)) \\ + g l_{50} m_5(\sin(q_1^* + q_2^* + q_3^* + q_4^*) - (q_1^* + q_2^* + q_3^* + q_4^*)\cos(q_1^* + q_2^* + q_3^* + q_4^*)) \end{bmatrix},$$

https://doi.org/10.1017/S0263574712000458 Published online by Cambridge University Press

$$B = \begin{bmatrix} -k & 0 \\ 0 & m_1(l_{01} + l_{10})g + (m_2 + m_3 + m_4 + m_5)(l_{01} + l_1)g \end{bmatrix},$$

$$C = \begin{bmatrix} \begin{array}{l} (l_{20}m_2 + l_2(m_3 + m_4 + m_5))\,(\cos(q_4^*) + q_4^* \sin(q_4^*)) + 2\,(l_{30}m_3 + l_3(m_4 + m_5))\,(\cos(q_3^* + q_4^*) \\ \quad + (q_3^* + q_4^*)\sin(q_3^* + q_4^*)) + 3\,(l_{40}m_4 + l_4m_5)\left(\cos(q_2^* + q_3^* + q_4^*) + (q_2^* + q_3^* + q_4^*)\sin(q_2^* + q_3^* + q_4^*)\right) \\ \quad + 4l_{50}m_5\left(\cos(q_1^* + q_2^* + q_3^* + q_4^*) + (q_1^* + q_2^* + q_3^* + q_4^*)\sin(q_1^* + q_2^* + q_3^* + q_4^*)\right) \\ 2l_4l_{50}m_5\left(q_1^*q_2^* + q_1^*q_3^* + q_1^*q_4^*\right)\sin(q_1^*) + 2l_3(l_{40}m_4 + l_4m_5)\left(q_2^*q_3^* + q_2^*q_4^*\right)\sin(q_2^*) \\ \quad + 2\,(l_2l_3(m_4 + m_5) + l_2l_{30}m_5)\,q_3^*q_4^*\sin(q_3^*) + 2l_3l_{50}m_5(q_1^*q_3^* + q_2^*q_3^* + q_1^*q_4^* + q_2^*q_4^*)\sin(q_1^* + q_2^*) \\ \quad + 2\,(l_2l_{40}m_5 + l_2l_4m_5)\left(q_2^*q_4^* + q_3^*q_4^*\right)\sin(q_2^* + q_3^*) + 2l_2l_{50}m_5\left(q_1^*q_4^* + q_2^*q_4^* + q_3^*q_4^*\right)\sin(q_1^* + q_2^* + q_3^*) \\ \quad + l_4l_{50}m_5\left(\sin(q_1^*) - q_1^*\cos(q_1^*)\right) + 2l_3l_{50}m_5\left(\sin(q_1^* + q_2^*) - (q_1^* + q_2^*)\cos(q_1^* + q_2^*)\right) \\ \quad + 3l_2l_{50}m_5\left(\sin(q_1^* + q_2^* + q_3^*) - (q_1^* + q_2^* + q_3^*)\cos(q_1^* + q_2^* + q_3^*)\right) + 4l_{50}m_5\,(l_{01} + l_1)\,(\sin(q_1^* + q_2^* + q_3^* + q_4^*) \\ \quad - (q_1^* + q_2^* + q_3^* + q_4^*)\cos(q_1^* + q_2^* + q_3^* + q_4^*)) + l_3\,(l_{40}m_4 + l_4m_5)\left(\sin(q_2^*) - q_2^*\cos(q_2^*)\right) \\ \quad + 2l_2\,(l_{40}m_4 + l_4m_5)\left(\sin(q_2^* + q_3^*) - (q_2^* + q_3^*)\cos(q_2^* + q_3^*)\right) \\ \quad + 3\,(l_{01}l_{40}m_4 + l_{01}l_4m_5 + l_1l_4m_5 + l_1l_{40}m_4)\sin(q_2^* + q_3^* + q_4^*) \end{array} \end{bmatrix},$$

$$D = \begin{bmatrix} 0 & 0 & 0 & 0 \\ gl_{50}m_5\cos(q_1^* + q_2^* + q_3^* + q_4^*) & \begin{array}{l} g\,(l_{40}m_4 + l_4m_5)\cos(q_2^* + q_3^* + q_4^*) \\ +gl_{50}m_5\cos(q_1^* + q_2^* + q_3^* + q_4^*) \end{array} & \begin{array}{l} g\,(l_{30}m_3 + l_3(m_4 + m_5)\cos(q_3^* + q_4^*) \\ +g(l_{40}m_4 + l_4m_5)\cos(q_2^* + q_3^* + q_4^*) \\ +gl_{50}m_5\cos(q_1^* + q_2^* + q_3^* + q_4^*) \end{array} & \begin{array}{l} g(l_{20}m_2 + l_2(m_2 + m_3 + m_4 + m_5))\cos(q_4^*) \\ +g\,(l_{30}m_3 + l_3(m_4 + m_5)\cos(q_3^* + q_4^*) \\ +g(l_{40}m_4 + l_4m_5)\cos(q_2^* + q_3^* + q_4^*) \\ +gl_{50}m_5\cos(q_1^* + q_2^* + q_3^* + q_4^*) \end{array} \end{bmatrix},$$

$$E = \begin{bmatrix} -4l_{50}m_5\sin(q_1^* + q_2^* + q_3^* + q_4^*) & \begin{array}{l} -3\,(l_{40}m_4 + l_4m_5)\sin(q_2^* + q_3^* + q_4^*) \\ -4l_{50}m_5\sin(q_1^* + q_2^* + q_3^* + q_4^*) \end{array} & \begin{array}{l} -2\,(l_{30}m_3 + l_3(m_4 + m_5))\sin(q_3^* + q_4^*) \\ -3\,(l_{40}m_4 + l_4m_5)\sin(q_2^* + q_3^* + q_4^*) \\ -4l_{50}m_5\sin(q_1^* + q_2^* + q_3^* + q_4^*) \end{array} & \begin{array}{l} -\,(l_2(m_3 + m_4 + m_5) + l_{20}m_2)\sin(q_4^*) \\ -2\,(l_{30}m_3 + l_3(m_4 + m_5))\sin(q_3^* + q_4^*) \\ -3\,(l_{40}m_4 + l_4m_5)\sin(q_2^* + q_3^* + q_4^*) \\ -4l_{50}m_5\sin(q_1^* + q_2^* + q_3^* + q_4^*) \end{array} \\ \begin{array}{l} I_5 + l_{50}^2m_5 - 2l_4l_{50}m_5\left(q_2^* + q_3^* + q_4^*\right)\sin(q_1^*) \\ -2l_3l_{50}m_5\left(q_3^* + q_4^*\right)\sin(q_1^* + q_2^*) \\ -2l_2l_{50}m_5q_4^*\sin(q_1^* + q_2^* + q_3^*) \\ +l_4l_{50}m_5\cos(q_1^*) + 2l_3l_{50}m_5\cos(q_1^* + q_2^*) \\ +3l_2l_{50}m_5\cos(q_1^* + q_2^* + q_3^*) \\ +4l_{50}m_5\,(l_{01} + l_1)\cos(q_1^* + q_2^* + q_3^* + q_4^*) \end{array} & \begin{array}{l} I_4 + I_5 + l_{40}^2m_4 + \left(l_4^2 + l_{50}^2\right)m_5 \\ -2l_3\,(l_{40}m_4 + l_4m_5)\left(q_3^* + q_4^*\right)\sin(q_2^*) \\ -2l_3l_{50}m_5\left(q_3^* + q_4^*\right)\sin(q_1^* + q_2^*) \\ -2l_2\,(l_{40}m_4 + l_4m_5)\,q_4^*\sin(q_2^* + q_3^*) \\ -2l_2l_{50}m_5q_4^*\sin(q_1^* + q_2^* + q_3^*) \\ +2l_4l_{50}m_5\cos(q_1^*) \\ +2l_3l_{50}m_5\cos(q_1^* + q_2^*) \\ +3l_2l_{50}m_5\cos(q_1^* + q_2^* + q_3^*) \\ +4\,(l_{01}l_{50} + l_1l_{50})\,m_5\cos(q_1^* + q_2^* + q_3^* + q_4^*) \\ +l_3\,(l_{40}m_4 + l_4m_5)\cos(q_2^*) \\ +2l_2\,(l_{40}m_4 + l_4m_5)\cos(q_2^* + q_3^*) \\ +3l_{01}\,(l_{40}m_4 + l_4m_5)\cos(q_2^* + q_3^* + q_4^*) \\ +3l_1\,(l_4m_5 + l_{40}m_4)\cos(q_2^* + q_3^* + q_4^*) \end{array} & \begin{array}{l} I_3 + I_4 + I_5 + l_{30}^2m_3 + l_3^2(m_4 + m_5) \\ +l_{40}^2m_4 + (l_4^2 + l_{50}^2)m_5 \\ -2l_2\,(l_3(m_4 + m_5) + l_{30}m_5)\,q_4^*\sin(q_3^*) \\ -2l_2\,(l_{40}m_4 + l_4m_5)\,q_4^*\sin(q_2^* + q_3^*) \\ -2l_2l_{50}m_5q_4^*\sin(q_1^* + q_2^* + q_3^*) \\ +2l_4l_{50}m_5\cos(q_1^*) \\ +2l_3l_{50}m_5\cos(q_1^* + q_2^*) \\ +3l_2l_{50}m_5\cos(q_1^* + q_2^* + q_3^*) \\ +4\,(l_{01}l_{50} + l_1l_{50})\,m_5\cos(q_1^* + q_2^* + q_3^* + q_4^*) \\ +2l_3\,(l_{40}m_4 + l_4m_5)\cos(q_2^*) \\ +2l_2\,(l_{40}m_4 + l_4m_5)\cos(q_2^* + q_3^*) \\ +3l_{01}\,(l_{40}m_4 + l_4m_5)\cos(q_2^* + q_3^* + q_4^*) \\ +3l_1\,(l_4m_5 + l_{40}m_4)\cos(q_2^* + q_3^* + q_4^*) \\ +2l_2\,(l_{30}m_3 + l_3(m_4 + m_5))\cos(q_3^*) \\ +2l_1\,(l_3(m_4 + m_5) + l_{30}m_3)\cos(q_3^* + q_4^*) \\ +2l_{01}\,(l_3(m_4 + m_5) + l_{30}m_3)\cos(q_3^* + q_4^*) \end{array} & \begin{array}{l} I_2 + I_3 + I_4 + I_5 + l_{20}^2m_2 \\ l_2^2(m_3 + m_4 + m_5) + l_{30}^2m_3 + l_3^2(m_4 + m_5) \\ l_{40}^2m_4 + l_4^2m_5 + l_{50}^2m_5 \\ +2l_4l_{50}m_5\cos(q_1^*) \\ +2l_3l_{50}m_5\cos(q_1^* + q_2^*) \\ +3l_2l_{50}m_5\cos(q_1^* + q_2^* + q_3^*) \\ +4\,(l_{01}l_{50} + l_1l_{50})\,m_5\cos(q_1^* + q_2^* + q_3^* + q_4^*) \\ +2l_3\,(l_{40}m_4 + l_4m_5)\cos(q_2^*) \\ +2l_2\,(l_{40}m_4 + l_4m_5)\cos(q_2^* + q_3^*) \\ +3l_{01}\,(l_{40}m_4 + l_4m_5)\cos(q_2^* + q_3^* + q_4^*) \\ +3l_1\,(l_4m_5 + l_{40}m_4)\cos(q_2^* + q_3^* + q_4^*) \\ +2l_2\,(l_{30}m_3 + l_3(m_4 + m_5))\cos(q_3^*) \\ +2l_1\,(l_3(m_4 + m_5) + l_{30}m_3)\cos(q_3^* + q_4^*) \\ +2l_{01}\,(l_3(m_4 + m_5) + l_{30}m_3)\cos(q_3^* + q_4^*) \end{array} \end{bmatrix}.$$

https://doi.org/10.1017/S0263574712000458 Published online by Cambridge University Press